CHAPTER SIX

Synthetic Biology-Based Solution NMR Studies on Membrane Proteins in Lipid Environments

Erik Henrich, Frank Löhr, Julija Mezhyrova, Aisha Laguerre, Frank Bernhard, Volker Dötsch[1]

Institute of Biophysical Chemistry, Centre for Biomolecular Magnetic Resonance, J.W. Goethe-University, Frankfurt am Main, Germany

[1]Corresponding author: e-mail address: vdoetsch@em.uni-frankfurt.de

Contents

Methods in Enzymology, Volume 614
ISSN 0076-6879
https://doi.org/10.1016/bs.mie.2018.08.019

Abstract

Although membrane proteins are in the focus of biochemical research for many decades the general knowledge of this important class is far behind soluble proteins. Despite several recent technical developments, the most challenging feature still is the generation of high-quality samples in environments suitable for the selected application. Reconstitution of membrane proteins into lipid bilayers will generate the most native-like environment and is therefore commonly desired. However, it poses tremendous problems to solution-state NMR analysis due to the dramatic increase in particle size resulting in high rotational correlation times. Nevertheless, a few promising strategies for the solution NMR analysis of membrane inserted proteins are emerging and will be discussed in this chapter. We focus on the generation of membrane protein samples in nanodisc membranes by cell-free systems and will describe the characteristic advantages of that platform in providing tailored protein expression and folding environments. We indicate frequent problems that have to be overcome in cell-free synthesis, nanodisc preparation, and customization for samples dedicated for solution-state NMR. Detailed instructions for sample preparation are given, and solution NMR approaches suitable for membrane proteins in bilayers are compiled. We further discuss the current strategies applied for signal detection from such difficult samples and describe the type of information that can be extracted from the various experiments. In summary, a comprehensive guideline for the analysis of membrane proteins in native-like membrane environments by solution-state NMR techniques will be provided.

1. INTRODUCTION

Within the last 20 years, techniques to characterize membrane proteins improved dramatically and especially examples of their structural investigation increased nearly exponentially (membrane proteins of known structure database: http://blanco.biomol.uci.edu/mpstruc/). The majority of known structures have been determined by X-ray crystallography and solution NMR spectroscopy, but with recent developments in detector technology the determination of high-resolution structures (Kühlbrandt, 2014) by cryo-EM is catching up. The drastic growth of structural data can be mainly attributed to improvements in measurement techniques and methodological advancements regarding protein production, purification, and sample preparation. High-end protein engineering (Serrano-Vega, Magnani, Shibata, & Tate, 2008), stabilization by small molecules or antibody fragments (Kim et al., 2015; Rasmussen et al., 2011, 2007), in meso crystallization (Caffrey, 2015), or lipid nanodiscs (Bayburt & Sligar, 2003) are only some of these developments. A general tendency is to focus on natural-like membrane environments for membrane protein research as more and more studies focus on

the role of lipids for membrane protein structure and stability (Barrera, Zhou, & Robinson, 2013; Gupta et al., 2017; Henrich et al., 2017; Saliba, Vonkova, & Gavin, 2015). In particular, the use of nanolipid particles as solubilization environment for membrane proteins in structural studies has set new standards (Denisov & Sligar, 2016; Efremov, Gatsogiannis, & Raunser, 2017; Nikolaev et al., 2017). This is not surprising as detergents can have a dramatic influence on the overall structural integrity or dynamics of membrane proteins (Dehez, Schanda, King, Kunji, & Chipot, 2017). Interestingly, the most preferred detergents for membrane solubilization and protein purification like *n*-dodecyl β-D-maltoside (He, Wang, & Yan, 2014) preserve a high amount of lipids still attached to the extracted membrane protein (Ilgü et al., 2014).

In this respect sample preparation techniques that avoid detergent contacts and allow subsequent analysis within natural membranes or membrane mimetics are desirable. Here, the cotranslational insertion of membrane proteins into defined membranes by synthetic approaches offers a remarkable advantage as any detergent contact is avoided during the direct folding of the nascent protein chain into a provided lipid bilayer (Harris et al., 2017). Nanodiscs are extremely well suited for this production process via cell-free expression systems (Roos et al., 2014). The extraordinary features and physicochemical properties of nanodiscs streamline protein purification and enable a sophisticated analysis by many state-of-the-art techniques (Denisov & Sligar, 2017). Control of the bilayer composition allows information about the effect of specific lipids (Dawaliby et al., 2016; Henrich et al., 2016; Rues, Dötsch, & Bernhard, 2016) or about the influence of general bilayer characteristics on membrane protein structure or stability (McClary, Sumida, Scian, Paço, & Atkins, 2016) to be obtained. In solution NMR spectroscopy, short-chain detergents have almost exclusively been used to provide a hydrophobic environment as they produce reasonable small particles that allow sufficiently fast tumbling. Bicelles were the first bilayer containing environment that gave high-resolution spectra of membrane proteins (Morrison et al., 2012). While they are widely used in solution NMR (Dürr, Gildenberg, & Ramamoorthy, 2012), their classical preparation still requires treatment of the solubilized membrane protein with detergent (Table 1). Nanolipoprotein particles only slowly found their entrance into the NMR field (Glück et al., 2009) since the first nanodiscs with a diameter of ~10 nm still were of unfavorable size (Denisov, Grinkova, Lazarides, & Sligar, 2004). Several recent improvements in nanodisc design (Hagn et al., 2013; Nasr et al., 2017) and sample preparation (Laguerre et al., 2016) initiated a broader usage of nanodiscs for solution NMR (Table 1).

Table 1 Strategies for Preparing Solution NMR Samples in Bilayer Environments

	Conventional		Cell-Free	
	Bicelles	**Nanodiscs**	**Nanodiscs**	**Bicelles**
Workflow	Cellular protein expression		Cell-free protein expression	
	Membrane solubilization		—	
	Purification		Purification	
	Reconstitution		—	
	—		—	Reverse *q*-titration
Preparation[a]	3–4 days	3–4 days	<24 h	<24 h
Detergent solubilization[b]	Yes	Yes	No	No
Detergent screen[c]	Membrane solubilization and purification		No	Reverse *q*-titration
Lipid selection	Synthetic and short-chain lipids		Any	Any
Particle size	~3–7 nm defined by *q*-ratio	~8–15 nm defined by MSP type	~8–15 nm defined by MSP type	Variable, defined by *q*-ratio
Label scrambling	Reduced by auxotrophic strains		Reduced by inhibitors	
Protocols and	Piai, Fu, Dev, and Chou (2017)	Hagn, Etzkorn, Raschle, and Wagner (2013)	Roos et al. (2014)	Laguerre et al. (2016)
Applications[d]	Morrison et al. (2012)	Bibow et al. (2014); Kofuku et al. (2014)	Lyukmanova et al. (2012)	

[a]Time estimates include all steps listed in the workflow section.
[b]Workflow requires complete solubilization of the membrane protein in detergent micelles.
[c]Workflow steps requiring detergent screening procedure.
[d]Selected references.

In this chapter, we describe the technical details of a complete pipeline from cell-free membrane protein production to NMR analysis in membrane environment. This involves the setup of customized cell-free protein production (Schwarz et al., 2007) allowing specialized labeling strategies (Hein, Löhr, Schwarz, & Dötsch, 2017; Laguerre et al., 2016; Löhr et al., 2012; Löhr, Tumulka, Bock, Abele, & Dötsch, 2015), the cotranslational

membrane protein insertion into defined nanodiscs (Henrich et al., 2016; Rues et al., 2016), and their transition into small bicelles for solution NMR measurements (Laguerre et al., 2016). The presented workflow will serve as a guideline to alleviate solution NMR characterizations of membrane proteins in native-like environments and potentially critical steps will be indicated.

2. BASIC CELL-FREE EXPRESSION SYSTEM

Expression systems based on cellular lysates have continuously been optimized for approximately the past 20 years. Systems utilizing lysates from different organisms including prokaryotic as well as eukaryotic sources (Kigawa et al., 2004; Madin, Sawasaki, Ogasawara, & Endo, 2000) are described and to some extent commercially available. Commercial systems are widely used and enable the quick access to cell-free technology, but they restrict options to optimize production and quality of the synthesized proteins. Individually prepared systems offer a more diverse variety of opportunities to adjust the expression conditions, as all supplemented components are known and under control (Schwarz et al., 2007). In addition, recent proteomics studies identified the residual protein components of *Escherichia coli* cell-free lysates obtained by standard preparation procedures (Foshag et al., 2018; Hurst et al., 2017). For economic reasons, tunable and most efficient protein synthesis, systems based on *E. coli* (Henrich, Hein, Dötsch, & Bernhard, 2015) or wheat germ (Harbers, 2014) cell lysates are thus currently recommended. *E. coli* is preferred for the on-site preparation of cell-free lysates as the preparation protocol and the quality of the lysate source are better controllable and more reliable.

2.1 *E. coli* Cell-Free Lysate Preparation

Various strains can be used as lysate source and the most common are *E. coli* A19 and BL21. Special applications may require engineered strains having, for example, eliminated release factors for the efficient incorporation of non-natural amino acids (Hong et al., 2014; Peuker et al., 2016). A standard S30 lysate preparation procedure out of a 10-L fermenter is described, which is able to provide 60–100 mL of cell-free lysate yielding 0.3–1.5 g of expressed protein (Foshag et al., 2018; Schwarz et al., 2007), but it should be noted that a variety of protocol modifications exist (Kigawa et al., 2004; Kim et al., 2006; Kwon & Jewett, 2015; Shrestha, Holland, & Bundy, 2012; Yang, Patel, Wong, & Swartz, 2012; Zubay, 1973):

1. Strike out *E. coli* A19 cells from a glycerol stock on a fresh agar plate and incubate the plate for 6–8 h. Inoculate two flasks containing 150 mL LB medium (10 g tryptone, 10 g NaCl, 5 g yeast extract/L) with the freshly grown cells and incubate them overnight at 37°C under vigorous shaking. The cultures usually grow to an OD_{600} of 6–7 overnight.
2. Inoculate 10 L of culture medium (16 g tryptone, 5 g NaCl, 10 g yeast extract/L) supplemented with 100 m*M* glucose and potassium phosphate buffer (22 m*M* KH_2PO_4, 40 m*M* K_2HPO_4) 1:66–100 with the preculture. At this stage, we recommend performing the cultivation in a fermenter to achieve higher cell densities and obtain a better yields and a higher quality of extract. It is also possible to use conventional culture flasks, but in our hands the lysate performance is reduced drastically. Cultivate the cells at 37°C under high oxygen saturation and stir until they reach mid-log phase (~4–5 OD_{600}) before cooling them down to ~18–20°C. The cooling step should not exceed 30 min. A growth curve should be recorded beforehand to assess the mid-log phase period in a given fermenter setup.
3. Cells are harvested by centrifugation (6700 × *g*, 20 min, 4°C) and the pellet is washed three times with 300 mL ice-cold buffer S30-A (10 m*M* Tris–acetate, pH 8.2, 14 m*M* $Mg(oAc)_2$, 60 m*M* KCl, 6 m*M* β-me) with 10 min centrifugation (8000 × *g*, 4°C) between the washes.
4. Pellet is resuspended in 110% (v/w) ice-cold buffer S30-B (10 m*M* Tris–acetate, pH 8.2, 14 m*M* $Mg(oAc)_2$, 60 m*M* KCl, 1 m*M* DTT, 1 × complete protease inhibitor) before cell breakage by a French Press device or similar automated cell breakage systems with standard settings for *E. coli*. The presented protocol recommends the cell breakage by mechanical force, but in general also sonication seems feasible (Shrestha et al., 2012).
5. Lysate is centrifuged at 30,000 × *g* for 30 min at 4°C. The supernatant is transferred to fresh tubes and the centrifugation step is repeated.
6. The supernatant is stepwise adjusted to 400 m*M* NaCl (5 *M* stock solution) before 45 min incubation at 42°C, which leads to a turbid solution.
7. The lysate is filled in dialysis bags (12–14 kDa MWCO) and dialyzed overnight at 4°C against 5 L buffer S30-C (10 m*M* Tris–acetate, pH 8.2, 14 m*M* $Mg(oAc)_2$, 60 m*M* KoAc, 0.5 m*M* DTT) with one buffer exchange after 3–4 h.
8. At the next day the lysate is centrifuged again (30,000 × *g*, 30 min, 4°C), split into aliquots and shock frozen with liquid nitrogen. The lysate can be stored at −80°C till usage and also can be shipped in lyophilized condition.

It should be noted that this procedure can be adapted to achieve desired lysate modifications, for example, to enhance the concentration of chaperones by an additional heat-shock step during the cultivation (Foshag et al., 2018). In this case, it should always be considered that any modification in lysate production may affect the production efficiency in subsequent cell-free protein production reactions (Foshag et al., 2018). By using appropriate blends, the advantages of lysates, e.g., giving high expression yields or improved folding by increased chaperone concentrations, can be combined (Rues, Dong, Dötsch, & Bernhard, 2018).

2.2 T7 RNA-Polymerase Preparation

The fast and efficient T7 RNA-polymerase is commonly employed for transcription within a coupled transcription and translation cell-free system (Schwarz et al., 2007). Since *E. coli* lysates still contain the endogenous RNA-polymerase (Foshag et al., 2018), cell-free reactions can alternatively be carried out with standard *E. coli* promotors and without the addition of T7 RNA-polymerase (Shin & Noireaux, 2010), but a significant drop in expression yield may occur. The following section illustrates the preparation of T7 RNA-polymerase by overexpression in *E. coli* cells (Schwarz et al., 2007). The yield of T7 RNA-polymerase out of 1 L *E. coli* culture is usually sufficient to supplement 0.5–1 L of cell-free lysate.

1. Inoculate an overnight culture (37°C, 200 rpm shaking) of LB medium (e.g., 150 mL) supplemented with 100 μg/mL ampicillin with BL21 (DE3) Star cells carrying the plasmid pAR1219 from a glycerol stock freshly grown on an agar plate.
2. Inoculate TB medium (12 g tryptone, 24 g yeast extract, 4 mL glycerol/L), 1–2 L is usually sufficient for a T7 RNA-polymerase batch, 1:100 (~0.1 OD_{600}) with the fresh overnight culture and incubate the culture at 37°C and 200 rpm shaking. When the OD_{600} reaches 0.6–0.8, induce T7 expression by the addition of 1 m*M* IPTG and incubate for further 5 h under the same conditions. Harvest the cells by centrifugation (6500 × *g*, 15 min, 4°C).
3. Resuspend the cells in 30 mL buffer (30 m*M* Tris–HCl, pH 8.0, 50 m*M* NaCl, 10 m*M* EDTA, 10 m*M* β-me, 5% (v/v) glycerol, 1 × complete protease inhibitors)/L of expression and sonicate eight times for 1 min with 30 s resting periods. Alternatively a French press can be used. Lysate is centrifuged (20,000 × *g*, 30 min, 4°C) and the supernatant is collected.

4. DNA is removed by the stepwise addition of 20% (w/v) streptomycin to a final concentration of 2%. Ensure incubation on ice and sufficient mixing after each step. DNA precipitate is removed by centrifugation (20,000 × *g*, 30 min, 4°C).
5. The supernatant is purified by anion exchange chromatography. The lysate is loaded on a Q-Sepharose column (75 mL bed volume for 1–2 L of expression culture), which was equilibrated with buffer A (30 m*M* Tris–HCl, pH 8.0, 50 m*M* NaCl, 1 m*M* EDTA, 10 m*M* β-me, 5% glycerol). After loading, the column is washed with buffer A until a stable baseline is reached. A gradient of 50–500 m*M* in 90 min (flow rate ~4 mL/min if allowed by pressure limit) is used for elution. Collect 2–3 mL fractions and analyze them by SDS-PAGE as elution profile might vary between runs. To save time the usage of gels enabling direct detection under UV is recommended. Combine fractions carrying high T7 RNA-polymerase concentrations (prominent band between 90 and 100 kDa). The T7 RNA-polymerase is not pure but sufficiently enriched after this step. Discard fractions with low concentrations and a high degree of impurities.
6. Dialyze collected fractions against 5 L buffer (10 m*M* K_2HPO_4, pH 8.0, 100 m*M* NaCl, 0.5 m*M* EDTA, 1 m*M* DTT, 5% glycerin) and afterward adjust the solution to 10% glycerol.
7. Concentrate the protein solution in Centriprep devices (50 kDa MWCO) by centrifugation (1500 × *g* for 10 min, 4°C) to a concentration of 2–4 mg/mL total protein. Adjust the concentrated samples to 50% glycerol and shock freeze in liquid nitrogen before storage at −80°C.
8. To determine the optimal amount of T7 RNA-polymerase for supplementation to cell-free reactions, perform a test cell-free reaction with increasing amounts of T7 polymerase. At a certain concentration a plateau is reached and the lowest T7 concentration of the plateau should be used for future reactions.

It is possible to skip this procedure by using commercially available T7 RNA-polymerase, but a concentration screen for obtaining the most efficient protein expression should be performed as well.

3. NANODISC PREPARATION

Nanodiscs are nanolipid particles that consist of a disc-shaped lipid bilayer, which is encircled by an ApoA1 derivative, the so-called membrane scaffold protein (MSP) (Fig. 1; Denisov & Sligar, 2017). The MSP protects the hydrophobic lipid tails and thus keeps the disc soluble.

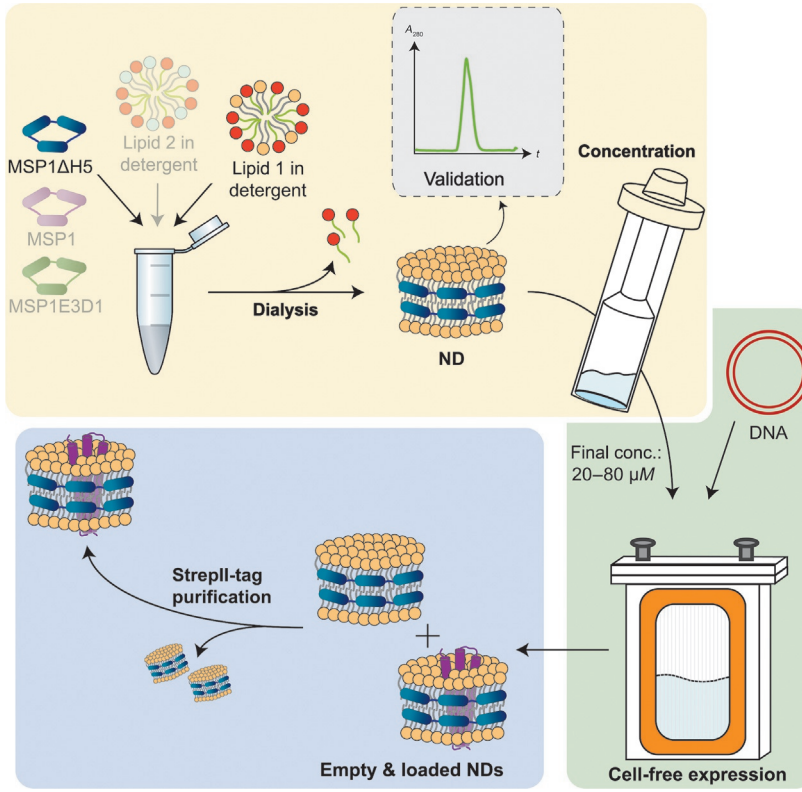

Fig. 1 General L-CF workflow including nanodisc formation (*yellow*), cell-free production (*green*) as well as sample purification (*blue*). Pictograms illustrate molecules or devices and workflow steps are indicated.

The reconstitution of "empty" nanodiscs (i.e., nonmembrane protein containing) as they are provided in cell-free reactions (Katzen et al., 2008; Roos et al., 2012) has been well established for more than 10 years (Bayburt, Grinkova, & Sligar, 2002; Denisov et al., 2004). Over the years engineered nanodiscs were designed for particular tasks, as, for example, nanodiscs with a smaller diameter that are more suitable for solution NMR experiments (Hagn et al., 2013). Particular comments and guidelines for successful nanodisc formation are given.

3.1 Preparation of Lipid Stock Solutions

For lipid stock solutions dedicated for nanodisc reconstitutions 50 m*M* is a reasonable concentration (Roos et al., 2014). The sufficient solubilization of the lipids is crucial for the successful reconstitution of a homogeneous

population of nanodiscs. As nanodiscs are formed upon detergent removal, detergents with a relatively high critical micellar concentration (cmc) are suitable as they can be easily removed from the mixture. Commonly the bile acid salt sodium cholate is used (Bayburt et al., 2002). In general, it is also possible to use other detergents, but detergents with a very low cmc can become problematic. Most lipids can be completely solubilized by 100 m*M* sodium cholate in water, but increased detergent concentrations should be considered if the solution still stays turbid. In this respect especially lipid mixtures extracted from natural sources can become problematic. Lipid stocks can be stored at −20°C.

3.2 MSP Preparation

The MSP can be produced by conventional expression in *E. coli* cells and purified via the N-terminal His_6-tag (Denisov et al., 2004). Thereby the same protocol is used for all different variants of MSP:

1. Freshly transform the selected MSP expression plasmid (Addgene) in BL21 (DE3) star cells, streak them out on an agar plate containing kanamycin and incubate the plate overnight at 37°C. Inoculate a 600-mL preculture of LB medium supplemented with kanamycin (30 μg/mL) and incubate overnight (37°C, 200 rpm shaking).
2. Inoculate LB medium (8 × 600 mL) supplemented with kanamycin (30 μg/mL) and glucose (0.5% (v/v)) with 50 mL of the grown overnight culture and incubate at 37°C and 200 rpm shaking until OD_{600} reaches 1–1.2. Induce MSP expression with 1 m*M* IPTG with additional incubation of 1 h at 37°C and 4 h at 28°C at 200 rpm shaking. Harvest the cells by centrifugation (6500 × *g*, 10 min, 4°C) and transfer the pellets to a falcon tube. Pellets can be stored at −20°C for few months or used directly for purification.
3. Resuspend cell pellet (~15–25 g) in 45 mL MSP-buffer (40 m*M* Tris–HCl, pH 8.0, 300 m*M* NaCl). Add 5 mL of a 10% Triton X-100 solution and gently mix the solution. Cell breakage is performed by sonication with 3 × 60 s and 3 × 45 s cycles with always 60 s resting time. Within the resting time ensure proper mixing. Centrifuge the suspension at 30,000 × *g* for 20 min at 4°C, collect the supernatant, and pass it through 0.45 μ*M* filters.
4. The filtered lysate is loaded on a His-trap column (bed volume ~20–25 mL) equilibrated with MSP-buffer supplemented with 1% Triton X-100. Afterward the column is washed with each five column

volumes of MSP-buffer with 1% Triton X-100, MSP-buffer at pH 8.9 containing additional 50 m*M* cholic acid, MSP-buffer, and MSP-buffer with addition of 50 m*M* imidazole. The protein is eluted by five column volumes of MSP-buffer containing additional 300 m*M* imidazole.

5. MSP-containing fractions are pooled and adjusted to 10% glycerol (v/v) before dialysis overnight against 5 L of MSP-buffer supplemented with 10% glycerol (v/v) with one buffer exchange after 3–4 h.

For some experiments it can be beneficial to label the MSP with heavy isotopes (Li, Kijac, Sligar, & Rienstra, 2006; Peetz et al., 2017). For labeling with ^{15}N and ^{13}C isotopes, LB overnight cultures are harvested by centrifugation (7000 × *g*, 10 min, 4°C) and resuspended in minimal media (2 g/L ^{13}C-glucose, 1 g/L ^{15}N-NH_4Cl, 0.2 g/L $FeCl_3$, 0.67 g/L $ZnCl_2$, 1 m*M* $MgSO_4$, 1 m*M* $CaCl_2$, 0.01 g/L thiamine, 0.1 g/L ampicillin, 3 g/L KH_2PO_4, 12.8 g/L Na_2HPO_4, 0.5 g/L NaCl). Expression is induced after 2 h at 37°C and 200 rpm shaking and the cultures are incubated for additional 3 h before harvesting (Peetz et al., 2017).

3.3 Nanodisc Reconstitution

For the formation of nanodiscs the MSP is first mixed with detergent-solubilized lipids (Fig. 1). It is crucial to consider previously defined MSP to lipid ratios for the formation of homogeneous discs (Marty, Wilcox, Klein, & Sligar, 2013; Roos et al., 2012). Due to the dilution of the lipid stocks it should be verified that the final detergent concentration is not reduced below its cmc. In that case either additional sodium cholate or *n*-dodecylphosphocholine (DPC) could be added to reach concentrations above cmc (Roos et al., 2012) or higher concentrated MSP stocks may be used. If the appropriate ratio of the selected lipid/MSP types is not known, a corresponding prescreen on an analytical scale (~100 μL samples) should be carried out. The samples are incubated with gentle shaking for about 1 h at temperatures above the lipid transition temperature, preferentially room temperature. Nanodisc formation is then induced by detergent removal with biobeads or by dialysis. For dialysis, a ~250 × volume (i.e., 5 L for 20 mL of mixture) of DF-buffer (40 m*M* Tris–HCl, pH 8.0, 100 m*M* NaCl) is recommended with incubation for 3 days and one buffer exchange each day. To separate the nanodiscs from soluble aggregates or aggregated lipids, the solution is centrifuged (22,000 × *g*, 20 min, 4°C) and the supernatant can be concentrated with DF-buffer equilibrated Centriprep tubes (10 kDa MWCO) by multiple centrifugation steps (20 min, 2000 × *g*, 4°C)

to a final concentration of 0.5–1 m*M* (Fig. 1). The concentrated solutions can be shock frozen by liquid nitrogen and stored at −80°C until usage.

3.4 Nanodisc Quality Control

The homogeneity of nanodisc stocks and the MSP:lipid ratio screens is analyzed by size-exclusion chromatography: 50 μL of a 20–50 μ*M* nanodisc solution is separated with an analytical size-exclusion column (e.g., Superdex 200 increase) in DF-buffer (Roos et al., 2012). Size and shape of prepared nanodiscs may be further evaluated by negative stain cryo-EM (Henrich et al., 2017). To prevent aggregation or extensive stacking on the grids, the nanodisc concentration should be kept ~20 μ*M*.

4. CELL-FREE INSERTION OF MEMBRANE PROTEINS INTO NANODISCS AND QUALITY OPTIMIZATION

In general, cell-free production approaches can be carried out in three major expression modes (Schwarz et al., 2007). The P-CF mode is performed without any supplied hydrophobic environment, but the resulting membrane protein precipitates can readily be solubilized in detergents. In the D-CF mode, detergents are supplied to the reaction leading to an immediate solubilization of the expressed protein. L-CF expressions contain bilayer structures such as liposomes, bicelles, or nanodiscs for membrane protein solubilization. Due to its simplicity and efficiency P-CF expression is usually the first choice for the production of a protein in a cell-free system, whereas the L-CF mode offers the opportunity to synthesize solubilized membrane proteins without any detergent contacts. Depending on the nature of the synthesized membrane protein, liposomes, bicelles, or nanodiscs might have different efficiencies for its proper cotranslational insertion and folding.

4.1 L-CF Expression

To setup a cell-free reaction, a variety of compounds responsible for energy supply (e.g., acetyl phosphate), a suitable chemical environment (e.g., Mg^{2+}, HEPES-buffer), precursors (e.g., amino acids), and preservation agents (e.g., protease inhibitors) are mixed together in a feeding mixture (FM), ensuring supply with nutrients as well as dilution of toxic byproducts. The FM is separated by a membrane from the reaction mixture (RM) holding the components responsible for transcription (e.g., T7 RNA-polymerase) and the protein production machinery (e.g., cell lysate). We highly recommend

the usage of such a continuous exchange setup with an RM to FM ratio of 1:15–20 to achieve an efficient production of material required for NMR experiments. The RM volume should be adjusted to the total amount of desired protein in the NMR sample and is usually between 1 and 10 mL. In Table 2 all ingredients with stock solution and final concentrations for the expression of an unlabeled protein are displayed and the required volumes for a 1-mL reaction with a 1:20 ratio of reaction to FM and a Mg^{2+} concentration of 18 m*M* are indicated. For preparative scale expressions in

Table 2 Compounds and Concentrations for a 1-mL Cell-Free Reaction

			Volume (µL)	
Compound	**Stock**	**Final**	**FM**	**RM**
RCWMDE[a]	16.67 m*M* each	1 m*M*	1200	60
20 Amino acids[b]	25 m*M* each	0.55 m*M* each	440	22
Acetyl phosphate	1000 m*M*	20 m*M*	400	20
Phosphoenolpyruvate	1000 m*M*	20 m*M*	400	20
NTP-mix[c]	75 ×	1 ×	266.7	13.3
DTT	500 m*M*	2 m*M*	80	4
Folinic acid	10 mg/mL	0.1 mg/mL	200	10
Complete cocktail[d]	50 ×	1 ×	400	20
HEPES-KOH (pH 8.0)/EDTA	2.5 *M*/0.5 *M*	100 m*M*/20 m*M*	800	40
$Mg(OAc)_2$	1000 m*M*	13.1 m*M*	262	13.1
KOAc	10,000 m*M*	110 m*M*	220	11
PEG8000	40%	2%	1000	50
Sodium azide	10%	0.05%	100	5
Addition to FM				
20 Amino acids[e]	25 m*M* each	0.5 m*M* each	400	
Buffer S30-C[f]	—	—	7000	
H_2O	—	—	6831	
Addition to RM				
[NDs (DMPG)][f]	750 µ*M*	100 µ*M*	133.3	
S30-Extract	100%	35%	350	

Continued

Table 2 Compounds and Concentrations for a 1-mL Cell-Free Reaction—cont'd

			Volume (μL)	
Compound	**Stock**	**Final**	**FM**	**RM**
Plasmid DNA	1 mg/mL	0.015 mg/mL	15	
RNAse inhibitor[g]	40 U/μL	0.30 U/μL	7.5	
T7-RNA polymerase[h]	3.63 mg/mL	0.03 mg/mL	5.5	
tRNA *E. coli*	40 mg/mL	0.50 mg/mL	12.5	
Pyruvate kinase	10 mg/mL	0.04 mg/mL	4	
H_2O	—	—	183.7	
Total volume			20,000	1000

[a]Is not added in protein-labeling reactions.
[b]For protein-labeling reactions adjust stock concentration to 30 mg/mL (total amino acid concentration) and final concentration to 1.5 mg/mL (total amino acid concentration) giving a final concentration of ~0.5 m*M* (each amino acid) in the RM.
[c]ATP, GTP, CTP, and UTP in the concentration of 360, 240, 240, and 240 m*M*, respectively.
[d]Protease inhibitor cocktail (one tablet in 1 mL H_2O, Roche Diagnostics).
[e]For labeled expressions adjust stock concentration to 30 mg/mL (total amino acid concentration) and final concentration to 0.5 mg/mL (total amino acid concentration). Together with the portion of amino acids from the general mix, which is used for the FM, this leads to a final concentration of ~0.6 m*M* (each amino acid) in the FM.
[f]Optional compound for L-CF expression with NDs, final concentration depends on target protein expression and its membrane insertion efficiency.
[g]Ribolock RNase inhibitor (Thermo Scientific).
[h]The stock and the final concentration of the T7-RNA polymerase varies from batch to batch and has to be determined in pilot experiments.
Adapted from Henrich, E., Dötsch, V., & Bernhard, F. (2015). Screening for lipid requirements of membrane proteins by combining cell-free expression with nanodiscs. *Methods in Enzymology, 556*, 351–369.

the mL range, the utilization of Slyde-A-lyzer devices with an MWCO of 10 kDa (Thermo Scientific) as container for the RM is very convenient. These are placed in special plastic containers that hold the FM (Schwarz et al., 2007). For screening purposes, smaller containers holding ~55 μL of RM are sealed with a dialysis membrane with an MWCO of 12–14 kDa fixed with a Teflon ring and then placed into standard 24-well cell culture plates holding 825 μL of FM. The basic steps for setting up preparative cell-free reactions are indicated here:

1. Stock solutions should be prepared in advance and stored at −20°C prior to usage. For salts and buffers 50 mL stocks and for amino acids 5–10 mL are suitable, whereas the other stock solutions may not exceed 2 mL due to lower stability of the compounds.
2. A premix of all low molecular weight components (Table 2, first section), which are present in the reaction as well as the FM, is prepared.

It is important to ensure proper mixing (at this step best performed by vortexing) before removing aliquots from the stock solutions (some stocks remain as suspensions) as well as after completing the premix.

3. The FM is completed by the addition of amino acids, buffer S30-C and H_2O (Table 2, second section). Mixing is performed by vortexing and the homogeneous FM is transferred to the reaction container.
4. The RM is completed by addition of the high molecular weight compounds (Table 2, third section). The completed RM is carefully mixed with a pipette. The membranes of the Slyde-A-lyzer are equilibrated from the outside with FM and then the RM is transferred into the Slyde-A-lyzer with a syringe. Excess air should be removed from the Slyde-A-lyzer to facilitate proper exchange of FM and RM.
5. Finally, the reaction container is closed and incubated under gentle shaking at 30°C for 12–20 h. After incubation, the RM is centrifuged at 16,000–20,000 × *g* for 10 min at 4°C to separate precipitates from the soluble fraction.

For protein-labeling experiments, the final amino acid concentration in the RM and FM should be adjusted to ~0.5–1 m*M* and ~0.6–1.5 m*M*, respectively, for each amino acid (Klammt et al., 2004; Löhr et al., 2015). Depending on the desired labeling, customized stock solutions, containing a fully labeled amino acid mix or a mixture of unlabeled and labeled amino acids, are required for specific experiments. For simplification, the amino acid stock solution can be prepared with a total amino acid concentration of 30 mg/mL giving 1.5 mg/mL of each amino acid. The final concentration in the RM and FM is in total 1.5 mg/mL and the extra shot for the FM is 0.5 mg/mL. Further detailed protocols for the setup of standard cell-free reactions including compound concentrations as well as dimensions of customized reaction containers have been described before (Henrich, Dötsch, & Bernhard, 2015; Klammt et al., 2004; Reckel et al., 2010; Schwarz et al., 2007).

For membrane protein solubilization the preformed nanodiscs are supplemented to the RM (Fig. 1 and Table 2) only. The suitable concentration as well as the type of nanodiscs (i.e., selected MSP type and lipid composition of the membrane) should be assessed in pilot experiments by considering the following points:

1. The MSP type should be selected according to the size of the membrane-integrated domains of the target protein to ensure an adequate size of the resulting nanodisc membrane. For solution-state NMR applications a rather short MSP type like MSP1D1ΔH5 is recommended as it forms

nanodiscs of only ~8 nm. This size is usually sufficient to accommodate most membrane proteins and even the formation of large assemblies such as the pentameric complex of the seven-transmembrane helix containing proton pump proteorhodopsin with a total molecular mass of ~135 kDa can be achieved (Peetz et al., 2017). On the other side, the limited membrane space can also hamper the insertion of specific membrane proteins or complexes. Thus, the expression of the target into different nanodisc types should be tested to evaluate the formation of soluble membrane protein/nanodisc complexes.

2. The composition of the bilayer should be customized to the protein of interest. Some proteins require a specific lipid environment for their functional fold and activity (Henrich et al., 2016). If a lipid dependency is not known, the insertion and subsequent analysis of the membrane protein into nanodiscs assembled with different lipids is recommended as an initial screen.
3. The nanodisc concentration should be adjusted to the target concentration in the reaction. Furthermore, individual membrane proteins strongly differ in their efficiency of nanodisc insertion (Roos et al., 2012). Screening different nanodisc concentrations (we recommend a range of 10–100 μ*M*) for an optimal solubilization should be considered and the lowest nanodisc concentration that achieves saturated solubilization is recommended for subsequent expression experiments. If multimeric proteins are analyzed, it should be taken into account that the nanodisc concentration can have an influence on the oligomeric state formation (Peetz et al., 2017). The oligomeric assembly of a protein in nanodiscs might be analyzed, e.g., by native mass spectrometry (Henrich et al., 2017).

Samples dedicated for NMR experiments require the supplementation of isotope-labeled amino acids. A fully labeled sample can be generated by specific mixtures containing all 20 amino acids with the desired isotopic labeling scheme (^{15}N, ^{13}C, and ^{2}H). Uniform labeling, however, can usually easily be achieved expression in *E. coli* in media containing ^{13}C-glucose or ^{15}N-ammonium chloride. The strength of cell-free expression is the ability to achieve specific labeling patterns due to control over the added amino acids and reduced metabolic scrambling (Reckel et al., 2010). Sophisticated labeling schemes facilitate the assignment of soluble as well as of membrane proteins (Hein et al., 2017; Löhr et al., 2012, 2015) and are described in detail in a recent review (Hoffmann, Löhr, Laguerre, Bernhard, & Dötsch, 2018). Moreover, residual amino acid scrambling can be addressed by the addition of distinct enzyme inhibitors (LaGuerre, Löhr, Bernhard, & Dötsch, 2015).

4.2 Customizing Cell-Free Expression Conditions

Since proteins fulfill numerous tasks in different environments, they exhibit a huge variety in structure and function. This diversity generates different demands on their surrounding environment or their interaction with other molecules. As protein folding depends on environmental factors, the open nature of cell-free systems is often a valuable benefit for the optimization of sample conditions (Fig. 2). For example, the addition of specific inhibitors (Laguerre et al., 2016) or cofactors (Waberer et al., 2017) can significantly enhance the general folding and stability of produced proteins. Furthermore, the correct formation of disulfide bridges, crucial for particular proteins, relies on redox conditions that in cell-free systems can be nicely adjusted to individual folding requirements (Rues et al., 2018). Increased concentrations of chaperones and other stabilizers can have a positive effect on protein folding (Foshag et al., 2018). While many diverse additives could be added to cell-free reactions, several issues need to be considered:

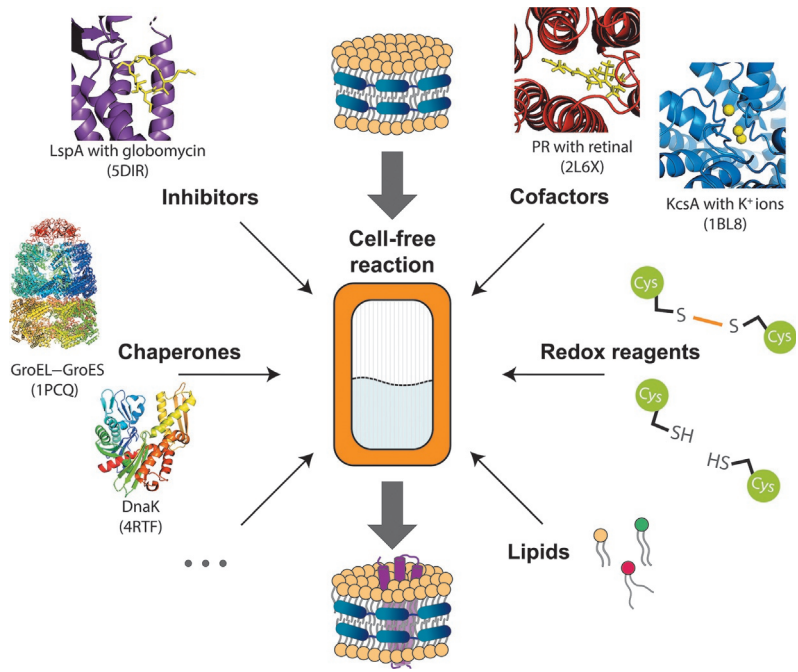

Fig. 2 Customizing cell-free expression conditions for improved sample quality. Protein structures are displayed with the corresponding PDB code. Cell-free device, lipids, nanodiscs, and redox systems are illustrated with pictograms.

1. The additive should be prepared in high stock concentrations as the available volume in the reaction is limited.
2. The pH of the additive should be similar to the pH in the reaction. Furthermore, the additive should not contain organic solvents. Exceptions can be ethanol or DMSO below 2% final concentration.
3. Potential negative effects of any new additive on the system should be tested in advance. Test expression screens of a reporter protein like GFP or luciferase, which enable a quick readout and covering different concentration ranges of the additive, are recommended.
4. It should be carefully considered if the additive can interfere with certain substances from the system. For example, Zn^{2+} supplementation requires the substitution of DTT with another reducing agent (e.g., TCEP; Waberer et al., 2017). In those cases the system has to be adapted before the additive tests.

4.3 Sample Purification

For NMR experiments, the purification of the target protein is necessary even in the reduced cell-free lysate proteome. In general, it is feasible to do NMR experiments directly from the RM of cell-free systems (Guignard, Ozawa, Pursglove, Otting, & Dixon, 2002). However, there is a high possibility that the resolution of the resulting spectra is decreased due to the viscosity of the RM and additional signals, which can arise due to conversion of labeled amino acids into other metabolites. To achieve suitable purity of membrane protein/nanodisc complexes, a one-step affinity purification by utilizing, e.g., His_6- or StrepII-tags is sufficient. As nanodiscs have a His_6-tag, using a different purification tag at the inserted membrane protein would remove empty discs (Fig. 1). Using StrepII-tagged membrane proteins is straightforward, while removing the His_6-tag from the nanodiscs by cleavage with TEV-protease would be an alternative option. The removal of empty discs from the sample significantly improves the resulting NMR spectra. In case of residual soluble aggregates, a final size-exclusion chromatography step can be added.

Suitable buffers for NMR experiments should have lower pH values to minimize signal loss due to amide protein exchange and low salt concentrations to ameliorate dielectric loss effects on the probe (e.g., 20 m*M* sodium acetate pH 4.0; 25 m*M* Bis–Tris pH 6.5; 20 m*M* potassium phosphate pH 7.2 (Laguerre et al., 2016; Peetz et al., 2017)). Exchange to such buffers can be done upon size-exclusion chromatography, by dialysis or during sample concentration by centrifugation in Amicon tubes with an MWCO of

10 kDa. Here, the concentration gradient within the tube should be considered. To prevent too high concentrations of the protein at the bottom of the tube, short centrifugation times (e.g., 5 min) should be applied, followed by removal of the filtrate and mixing of the concentrated solution. Buffer exchange during concentration can be achieved by multiple dilutions of the concentrated sample with the new buffer and subsequent concentration. At this state it can be highly beneficial to first screen various buffers with gradually lower pH for their suitability.

5. BASIC NMR SAMPLE PROCESSING AND ANALYSIS

Structure determination of membrane proteins by solution NMR is a general challenge and most so far studies were performed with proteomicelles (Liang & Tamm, 2016). While detergent micelles frequently represent a stabilizing environment similar to membranes (Hagn et al., 2013), a variety of membrane proteins strictly require lipid contacts (Henrich et al., 2016). Moreover, detergents suitable for solution-state NMR may drastically alter protein dynamics (Dehez et al., 2017; Kurauskas et al., 2018). The previous chapters focused on the workflow of sample preparation based on cell-free expression in the presence of supplied nanodiscs, with the option of subsequent bicelle formation by reverse q-titration as outlined in the next paragraph. The experiments described in Sections 5–7 can be performed with either bicelles or nanodiscs and are independent of the employed sample preparation procedure. Conventional cell-based expression systems might thus be considered if a membrane protein is sufficiently synthesized, can efficiently be labeled with stable isotopes, and tolerates detergent extraction from the membrane. An overview on the different sample production strategies is given in Table 1.

5.1 Environment and Interactions

Structure, function, and stability of membrane proteins are drastically modulated by their hydrophobic environment, making the identification of a suitable solvation agent a crucial task. While in the past usually a variety of different detergents were only screened for giving good spectral resolution, the increasing variety of solvation agents now includes also other membrane mimetics or amphipols (Etzkorn et al., 2013). Any hydrophobic environment must be evaluated for its spectral resolution (Etzkorn et al., 2013; Frey, Lakomek, Riek, & Bibow, 2017), but effects on structural state and functional behavior should be assessed as well by orthogonal studies like

activity assays (Etzkorn et al., 2013; Laguerre et al., 2016). For the spectral assessment, ^{15}N HSQC experiments are commonly performed to define the general number of signals and their distribution (Fig. 3A). This type of experiments is highly advantageous as it can be performed with even quite low sample concentrations in the order of 100 μM. Unfavorable line broadening of membrane protein samples can be addressed by applying transverse relaxation-optimized spectroscopy (TROSY)-type experiments (Pervushin, Riek, Wider, & Wüthrich, 1997). For the acceleration of the data collection the band-selective excitation short-transient (BEST) pulse sequence should be applied as well (Schanda, Van Melckebeke, & Brutscher, 2006).

Classical chemical shift studies will identify protein/ligand interactions upon ligand titration. The spectral comparison of apo and holo protein can reveal information about binding sites, protein dynamics, and conformational changes (Fig. 3B). If the chemical shift dispersion of the spectra is sufficient, these experiments can be performed on fully labeled samples (Laguerre et al., 2016). Using nanodiscs can involve the problem of signal overlap due to the size of the particle. In these cases, a smaller bicelle environment, that still comprises a lipid bilayer, can be generated by reverse q-titration (Laguerre et al., 2016). This is achieved by the stepwise titration of detergents like DPC or 1,2-diheptanoyl-*sn*-glycero-3-phosphocholine (DH^7PC) into the nanodisc sample, which breaks up the nanodisc particle, leaving particles with a smaller size and thus with faster tumbling. The progress of signal improvement and the lipid/detergent concentrations can be monitored by TROSY and 1D spectra, respectively. To prevent a substantial dilution of the sample, detergent stock concentrations should be around 10% (w/v). For elevated molecular weight proteins, which usually display an even more severe signal overlap, amino acid-type-selective labeling, potentially also focusing on methyl groups by methionine (Kofuku et al., 2012; Nygaard et al., 2013) or valine (Isogai et al., 2016), represents another possibility to simplify the analysis. Extremely large complexes like GPCRs incorporated into nanodiscs will require in addition the production of deuterated samples (Kofuku et al., 2014).

5.2 ^{31}P NMR

Like nanodiscs, bicelles are small disc-like membrane patches that in contrast to the former are not stabilized by an amphipathic protein, but by detergent molecules. They are typically formed by short-chain lipids such as

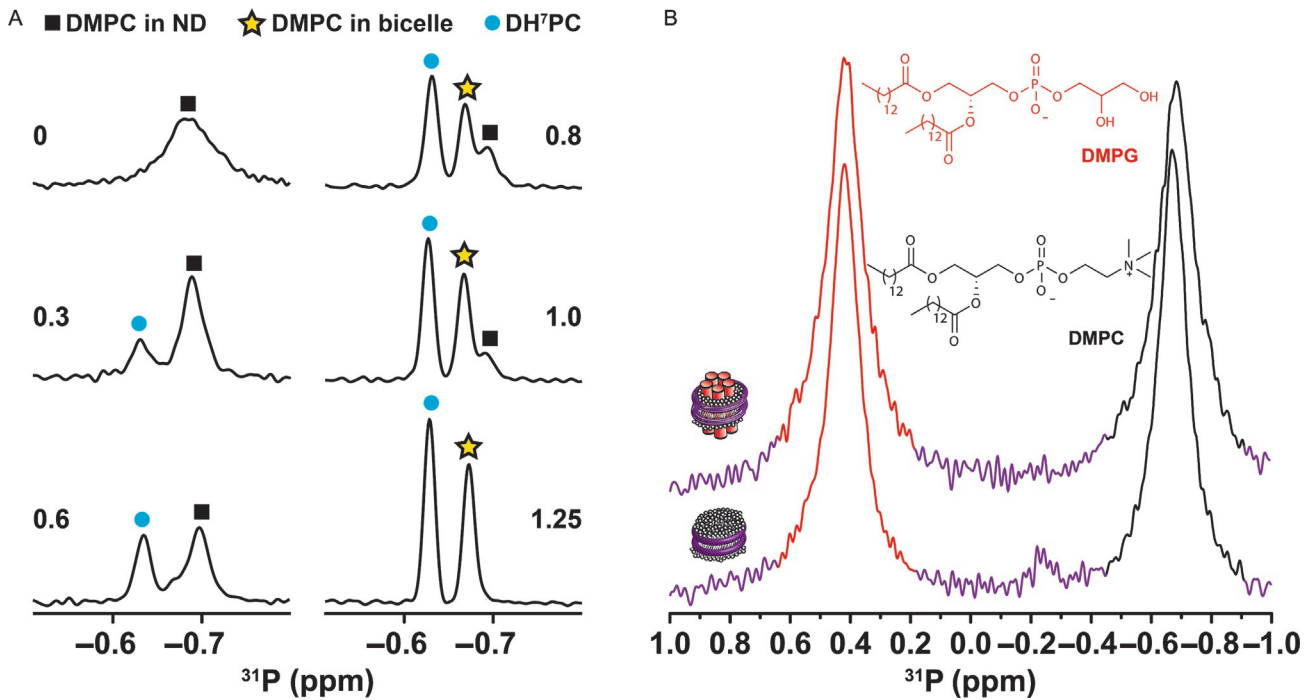

Fig. 3 $^{15}N,^{1}H$-TROSY of LspA in different conditions. The influence of different hydrophobic environments on LspA is demonstrated in (A). In (B) the stabilization of LspA by the inhibitor globomycin is shown. The color-codes of the spectra are indicated in the legends. *Adapted from Laguerre, A., Löhr, F., Henrich, E., Hoffmann, B., Abdul-Manan, N., Connolly, P. J., et al. (2016). From nanodiscs to isotropic bicelles: A procedure for solution nuclear magnetic resonance studies of detergent-sensitive integral membrane proteins.* Structure, 24*(10), 1830–1841.*

1,2-dimyristoyl-*sn*-glycero-3-phosphocholine (DMPC) or 1,2-dimyristoyl-*sn*-glycero-3-phospho-(1-rac-glycerol) (DMPG) with DH^7PC, DPC or 3-[(cholamidopropyl)dimethylammonio]-1-propanesulfonate (CHAPS) ensuring the solubilization. In first experiments, the size and composition of a desired bicelle are adjusted by defining the optimal ratio between lipids and detergents, the so-called *q*-value (1):

$$q = \frac{[\text{lipid}]}{[\text{detergent}]} \tag{1}$$

In the case of bicelle generation from membrane protein/nanodisc complexes, here referred as "reverse *q*-titration," we use the reciprocal *q*-value (2):

$$q^{-1} = \frac{[\text{detergent}]}{[\text{lipid}]} \tag{2}$$

At known lipid concentrations, the *q*-value can easily be adjusted by supplying appropriate detergent concentrations. However, absolute concentrations are often unknown and then NMR analysis offers an easy tool for the determination of the *q*-value by detecting the naturally NMR active phosphorus nucleus (^{31}P) of lipids in 1D-^{31}P experiments. Similarly, phosphate-containing detergents like DH^7PC or DPC can be detected (Fig. 4A). By calculating the integrals of NMR signals arising from either lipid or detergent the *q*-value can be defined. Due to the large chemical shift anisotropy (CSA) contribution to transverse relaxation, best resolution is often obtained with low field spectrometers. In case of phosphate-free detergents such as cholesterol or CHAPS, the NMR quantification, e.g., by detection of ^{13}C nuclei, can be problematic due to the possible overlap with protein resonances. Peak overlap might also prevent the distinction between DPC or DH^7PC and particular lipids. Here, a calculation of the added amounts is indispensable. Interestingly, in the case of reverse *q*-titration the transition of nanodiscs into bicelles can be followed and estimated by a correlated peak splitting and downshift of the lipid signals (Laguerre et al., 2016). By quantifying the lipid amount inside nanodiscs before and after the cotranslational insertion of a membrane protein, the release of lipids from the bilayer and the membrane area occupied by the inserted protein can be estimated (Peetz et al., 2017). The NMR quantification of ^{31}P-containing lipids can therefore serve as a valuable future tool to characterize lipid mixtures, membrane protein dimensions, or general changes of nanoparticle topologies (Fig. 4B).

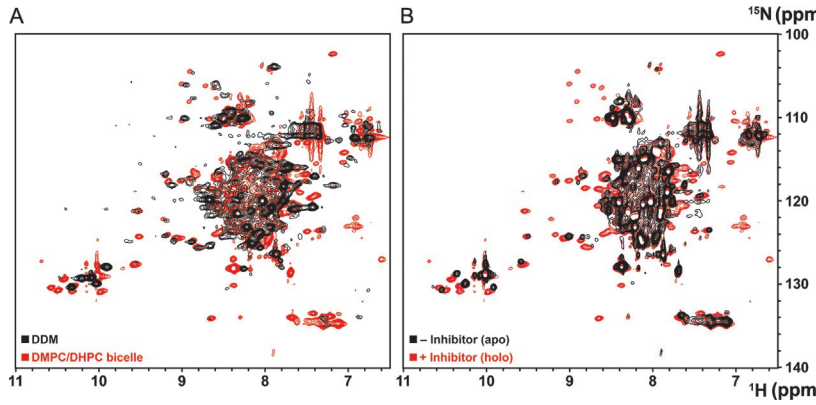

Fig. 4 1D-^{31}P NMR of nanodiscs. 1D-NMR spectra of the reverse *q*-titration with the detergent DH^{7}PC of nanodiscs assembled with MSP1D1ΔH5 and DMPC are shown in (A). Peaks of different species are highlighted with symbols (see legend) and *q*-ratios are displayed. (B) 1D-NMR spectra of nanodiscs formed by MSP1D1ΔH5 with an equimolar mixture of DMPG and DMPC before (*lower curve*) and after the insertion of proteorhodopsin (*upper curve*). The chemical structures of the lipids are displayed and the corresponding peaks are highlighted in *matched colors*. Pictograms illustrate the analyzed particles. Spectra (A, B) were recorded at 202 MHz and a sample temperature of 318 K on a Bruker DRX500 spectrometer equipped with a broadband inverse probe. *Panel (A): Adapted from Laguerre, A., Löhr, F., Henrich, E., Hoffmann, B., Abdul-Manan, N., Connolly, P. J., et al. (2016). From nanodiscs to isotropic bicelles: A procedure for solution nuclear magnetic resonance studies of detergent-sensitive integral membrane proteins.* Structure, 24*(10), 1830–1841.*

5.3 TRACT

The definition of particle size is highly desirable as significant variations exist among membrane proteins due to attached hydrophobic molecules (Ilgü et al., 2014). Therefore, TRACT (TROSY for rotational correlation times) measurements giving a fast approximation of rotational correlation times represent a perfect tool (Lee, Hilty, Wider, & Wüthrich, 2006). It should, however, be noted that the true correlation time of membrane protein can be severely underestimated if the entire amide region is chosen for integration in 1D spectra, because already a small number of mobile residues or side-chain signals may contribute a large portion to the total integrals. In favorable cases, e.g., with β-barrel proteins or α-helical proteins featuring well-dispersed amide signals, suitable regions may be selected easily.

Alternatively, selectively labeled samples may be used for 1D TRACT analysis, allowing it to obtain residue-specific τ_c values from resolved signals (Etzkorn et al., 2013). Although more time consuming, 2D TRACT

versions are in general advantageous in this respect as they allow single signals or groups of signals from structured regions of the protein to be selected for integration in a straightforward manner using uniformly labeled samples (Laguerre et al., 2016). Here, differential observations for single amino acids can be made that provide single residue mobility information allowing for estimations regarding membrane partitioning or involvement in specific protein motions.

6. BACKBONE ASSIGNMENT OF MEMBRANE PROTEINS

The unfortunate coincidence of inherently low chemical shift dispersion and slow rotational reorientation of membrane proteins—in particular in lipid-like environments—renders their resonance assignment by solution NMR techniques challenging (Kim, Howell, Van Horn, Jeon, & Sanders, 2009; Maslennikov & Choe, 2013; Sanders & Sönnichsen, 2006; Viegas, Viennet, & Etzkorn, 2016). Routinely used 3D experiments for backbone assignment rely on matching ^{13}C chemical shifts observed in intra- and interresidual correlations with amide ^{1}H and ^{15}N resonances. This procedure is severely compromised by spectral crowding in the NH plane as well as ^{13}C chemical shift degeneracy caused by the prevalence of one secondary structure type and the high abundance of certain amino acid types in transmembrane regions (Reckel et al., 2008). Long rotational correlation times entail fast transverse relaxation which translates into broad resonances and inefficient magnetization transfer. In addition, exchange between different environments and interconverting conformations at a timescale in the order of the frequency difference of the corresponding resonances may lead to excessive line broadening.

Although the effect of high molecular mass of samples is alleviated to some extent by the use of TROSY, perdeuteration at nonexchangeable sites, and high measurement temperatures, the performance of crucial experiments, such as HNCACB (Wittekind & Mueller, 1993), HN(CO)CACB (Yamazaki, Lee, Arrowsmith, Muhandiram, & Kay, 1994), or HN(CA)CO (Clubb, Thanabal, & Wagner, 1992) that involve ^{13}C–^{13}C transfer steps, is severely hampered for ordered residues in membrane proteins (Etzkorn et al., 2013; Laguerre et al., 2016; Löhr et al., 2012, 2015; Schubert, Kolbe, Kessler, Oesterhelt, & Schmieder, 2002). On the other hand, exclusively relying on C^{α} connectivities resulting from the more sensitive HNCA (Ikura, Kay, & Bax, 1990) and HN(CO)CA (Bax & Ikura, 1991) experiments is usually insufficient and requires additional information to resolve

ambiguities. In principle such information can be obtained from amino-acid-type-selective triple-resonance experiments (Dötsch, Oswald, & Wagner, 1996; Feuerstein, Plevin, Willbold, & Brutscher, 2012; Pantoja-Uceda & Santoro, 2008; Schubert, Smalla, Schmieder, & Oschkinat, 1999) which are, however, unsuitable for large proteins due to their multistep coherence transfer or editing elements. Alternatively, amino acid-type-specific isotope labeling (Griffey, Redfield, Loomis, & Dahlquist, 1985; LeMaster & Richards, 1985; Muchmore, McIntosh, Russell, Anderson, & Dahlquist, 1989; Senn, Eugster, Otting, Suter, & Wüthrich, 1987) provides valuable assignment information in a very sensitive manner and leads to substantial spectral simplifications. The simultaneous use of both, ^{15}N- and 1-^{13}C (carbonyl)-labeled amino acid types, results in sequence-specific backbone NH assignments for unique amino acid pairs by exploiting the scalar ^{13}C–^{15}N coupling across the peptide bond (Griffey, Redfield, McIntosh, Oas, & Dahlquist, 1986; Guignard et al., 2002; Ikura, Krinks, Torchia, & Bax, 1990; Kainosho & Tsuji, 1982; Takahashi et al., 1991; Tate et al., 1992; Weigelt, van Dongen, Uppenberg, Schultz, & Wikström, 2002; Westler et al., 1988; Yabuki et al., 1998). Since the latter interaction is relatively strong and can be detected in a straightforward manner, this assignment strategy has been applied for larger proteins (Kato et al., 1989; Rule, Tjandra, Simplaceanu, & Ho, 1993). On the downside, the use of these strategies to identify all residue types or even all amino acid pairs occurring in a protein would require preparation of a prohibitively large number of labeled samples. The same goal can, however, be achieved with considerably higher efficiency using combinatorial methods (Hefke et al., 2011; Parker, Aulton-Jones, Hounslow, & Craven, 2004; Shortle, 1994; Staunton, Schlinkert, Zanetti, Colebrook, & Campbell, 2006; Wu et al., 2006).

Combinatorial amino acid-selective labeling (see Hoffmann et al., 2018; Jaipuria, Krishnarjuna, Mondal, Dubey, & Atreya, 2012 for recent reviews) employs a limited number of samples, each containing different subsets of labeled amino acids rather than a single labeling type per sample. In an early application of dual-selective combinatorial ^{15}N- and 1-^{13}C-labeling to a detergent-solubilized membrane protein (Trbovic et al., 2005), ^{15}N HSQC and 2D HN(CO) spectra recorded on a set of three samples provided amino-acid-type information and sequence-specific assignments that served as "anchor points" to facilitate the classical 3D-based approach, finally resulting in 85% overall backbone assignment. As mentioned earlier, some important 3D triple-resonance experiments fail for large protein/lipid complexes. It is therefore desirable to increase the information content of a combinatorial

labeling scheme such that finally only short gaps in the protein sequence have to be filled that can be assigned with the most sensitive 3D experiments recorded on a uniformly labeled sample. Three options are conceivable to achieve this goal: (1) increasing the number of samples, (2) use of multiple ^{15}N and ^{13}C enrichment levels, and (3) introducing more isotopomerically distinct dipeptide species. The first approach has been successfully employed to assign a number of proteins containing two to four transmembrane helices with the help of up to eight dual-selectively labeled samples (Maslennikov et al., 2010). The second method allows the distinction of all 19 nonproline amino acid types with as few as 3 samples and requires evaluation of signal intensities to decode enrichment levels (Kasai, Koshiba, Yokoyama, & Kigawa, 2015). Taking into account the large dynamic range of signal intensities often observed in membrane protein spectra, the latter issue may be critical at some instances. Implementation of the third option can be achieved by labeling amide nitrogens, carbonyl carbons, and α-carbons individually as well as simultaneously in different amino acid types of the same sample (Löhr et al., 2012, 2015). In this combinatorial triple-selective labeling strategy, sample preparation efforts are reduced at the expense of a larger variety of 2D $^{1}H–^{15}N$ correlation experiments that need to be carried out per sample in order to distinguish more amino-acid-type pairs based on their distinct labeling patterns. Nevertheless, the required set of spectra can usually be acquired in a reasonable amount of time especially when applying time-shared pulse sequences (Hein et al., 2017; Löhr et al., 2014). It should however be noted that despite the higher sensitivity of the latter experiments compared to 3D triple-resonance experiments comprising ^{13}C evolution times, application to slowly tumbling protein complexes still requires the use of deuterated amino acids (Laguerre et al., 2016).

7. NMR STRUCTURAL APPROACHES FOR MEMBRANE PROTEINS IN LIPID BILAYERS

7.1 Distance Restraints

The most important source of structural information of biomolecules in solution NMR is the nuclear Overhauser effect (NOE). For slowly tumbling proteins the collection of NOE-based distance constraints is to a large extent confined to methyl groups. Together with aromatic rings these are involved in forming the hydrophobic cores, and in membrane proteins methyl-containing amino acids are highly abundant in transmembrane regions. Being located at the end of the side chains methyl groups feature

increased local mobility compared to other side-chain or backbone positions, thus diminishing linewidth limitations. In addition, fast rotation around the carbon–carbon bond makes the methyl protons chemically equivalent, resulting in threefold enhanced signal intensities. Spectroscopically, significant line narrowing can be achieved by virtue of cancellation of intramethyl ^{1}H–^{1}H and ^{1}H–^{13}C dipolar relaxation mechanisms (Ollerenshaw, Tugarinov, & Kay, 2003; Tugarinov, Hwang, Ollerenshaw, & Kay, 2003) when using of HMQC-type pulse sequences (methyl-TROSY). The effect is most pronounced when the influence of external dipolar relaxation sources is minimized such as in side chains containing a single-protonated, ^{13}C-labeled methyl group, whereas all other sites are deuterated but not ^{13}C labeled (Tugarinov & Kay, 2004). At the same time, such a labeling scheme eliminates signal broadening due to passive scalar couplings. Most importantly, the absence of $^{1}J_{CC}$ couplings allows for enormous resolution gains without reverting to low-sensitivity constant-time methods. Protein sample production involves either incorporation of methyl-labeled amino acids (Miyanoiri et al., 2013) in *E. coli* cellular or cell-free expression systems or, more commonly, α-ketoacid precursor-based cellular expression using deuterated minimal media (Gardner & Kay, 1997; Goto, Gardner, Mueller, Willis, & Kay, 1999; Hagn & Wagner, 2015; Lichtenecker, Coudevylle, Konrat, & Schmid, 2013; Tugarinov, Kanelis, & Kay, 2006). High label costs and insufficient precursor conversion can be addressed by a recently developed new strategy based on the methyl side-chain labeling of proteins by cell-free synthesis using amino acid precursors (Lazarova et al., 2018). Special *E. coli* lysates enriched with the branched chain aminotransferase IlvE showed almost complete conversion of the labeled precursors 2-ketoisovaleric acid (KIV) or 4-methyl-2-oxovalerate (MOV) to methyl-labeled L-Val or L-Leu. Besides a tremendous reduction in label costs, additional advantages are the options to exclusively label either L-Val or L-Leu methyl residues, the lack of any precursor scrambling and to preserve high production efficiencies of even complex membrane proteins.

Taking into account the above considerations the most useful setup for the measurement of NOEs in membrane protein/lipid complexes is the application of HMQC–NOESY–HMQC-type pulse sequences (Clore, Kay, Bax, & Gronenborn, 1991; Frenkiel, Bauer, Carr, Birdsall, & Feeney, 1990; Kay, Clore, Bax, & Gronenborn, 1990; Vuister et al., 1993; Zuiderweg, Petros, Fesik, & Olejniczak, 1991) to selectively ^{15}N- and $^{1}H/^{13}C$-methyl-labeled samples in a $^{2}H/^{12}C$ background—a combination which provides the highest achievable sensitivity and resolution. The purpose

of ^{15}N labeling is the sequence-specific assignment of methyl resonances by virtue of intraresidual amide-to-methyl NOE contacts detected in ^{15}N,^{13}C-separated HMQC–NOESY–HMQC variants. Here, it should be noted that for slowly tumbling molecules the [^{1}H–^{15}N]-HMQC module takes advantage of relaxation interference between ^{1}H CSA and ^{1}H–^{15}N dipolar mechanisms ("CRINEPT–HMQC–[^{1}H]-TROSY" (Riek, Wider, Pervushin, & Wüthrich, 1999)) allowing for the use of magnetization transfer periods that are considerably shorter than the nominal $1/(2 * {}^{1}J_{NH})$ duration, thus minimizing relaxation losses. In a second set of experiments, ^{13}C,^{13}C-separated HMQC–NOESY–HMQC spectra are acquired in order to obtain interresidue methyl–methyl distance information. Although more time consuming, it may be advisable to record 3D (two experiments incorporating either ^{1}H or ^{13}C evolution times before NOE mixing) as well as 4D (with both evolution times) versions. The 3D versions are more sensitive and can be recorded with the conventional, full sampling method. Therefore, all NOE cross-peaks that can potentially be detected for a given system should be present in the 3D spectra. However, being spread along a single indirect dimension, only a small fraction of the donor methyl resonances can usually be assigned without prior structural information. Owing to the dispersion along two indirect dimensions, vastly removing overlap, and the fact that donor ^{1}H and ^{13}C chemical shifts are directly correlated, their four-dimensional counterparts can in principle provide NOE assignments in an unambiguous manner. On the other hand, lower sensitivity and possibly artifacts arising from restricted phase cycling or sampling (see later) may raise doubts about the reliability of an observed cross-peak. In such cases, it is helpful to verify the putative NOE by the presence of cross-peaks at the corresponding coordinates in the 3D spectra.

In order to exploit the full potential of resolution optimized methyl-selective labeling schemes, long acquisition times must be employed in all indirect dimensions of an NOESY experiment. In the case of 4D experiments, this would require unmanageable long periods of measurement time (in the order of months to years). Therefore, nonuniform sampling schemes (Holland, Bostock, Gladden, & Nietlispach, 2011; Mobli & Hoch, 2014; Orekhov, Ibraghimov, & Billeter, 2003; Sun, Frueh, Selenko, Hoch, & Wagner, 2005; Zawadzka-Kazimierczuk, Kazimierczuk, & Koźmiński, 2010), where only a few percent of the full time-domain data grid is actually sampled, are now routinely used to obtain high-resolution 4D NOESY spectra (Hiller, Ibraghimov, Wagner, & Orekhov, 2009; Luan, Jaravine, Yee, Arrowsmith, & Orekhov, 2005; Orekhov & Jaravine, 2011; Reckel et al., 2011; Stanek et al., 2013; Werner-Allen, Coggins, & Zhou, 2010).

Moderate sensitivity gains can sometimes be realized by sampling more data points at short evolution time values, where intensities are comparatively high, and fewer points are present at later stages of the interferograms (Barna & Laue, 1987; Rovnyak, Hoch, Stern, & Wagner, 2004; Schmieder, Stern, Wagner, & Hoch, 1993).

Significant time savings and/or sensitivity improvements in HMQC-type experiments can also be accomplished by the use of band-selective proton pulses in combination with small flip angles (SOFAST-HMQC), as demonstrated for amide $^{1}H–^{15}N$ (Schanda & Brutscher, 2005) as well as for methyl $^{1}H–^{13}C$ correlations (Amero et al., 2009). Likewise, HMQC–NOESY–HMQC experiments can be implemented to benefit from the underlying longitudinal relaxation enhancement (Rossi, Xia, Khanra, Veglia, & Kalodimos, 2016). In our experience application of such pulse sequences to membrane proteins often suffer from extensive t_1-noise in the aliphatic region, especially if nondeuterated lipids or detergents have been employed for NMR sample preparation. Such artifacts can however be avoided by the use of a gradient-echo/antiecho coherence selection scheme (Davis, Laue, & Keeler, 1991). Although this modification degrades sensitivity by a theoretical factor of $2^{1/2}$, it is finally the signal-to-artifact ratio that is more relevant for obtaining reliable NOE information than the signal-to-(white) noise ratio.

Besides typical distance restraints generated by NOEs the introduction of spin probes, usually by coupling of paramagnetic spin labels to specific cysteine mutants, can deliver additional information. These paramagnetic relaxation enhancement (PRE) experiments can be complementary to NOE information, provide distance information in the range of 15–24 Å (Liang, Bushweller, & Tamm, 2006), and have been used for structural determinations of membrane proteins from various types (Hagn et al., 2013; Reckel et al., 2011). The efficient incorporation should be checked by MS or EPR spectroscopy to guarantee uniform labeling. Unlabeled protein would decrease the overall PRE effect and thus lead to inaccurate distance restraints. For the visualization of the PRE effect [^{15}N,^{1}H]-TROSY–HSQC spectra of diamagnetic and paramagnetic labeled proteins are recorded and compared. Signals of residues affected by the paramagnetic probe are reduced compared to diamagnetic conditions and the distance of the residue toward the probe can be back calculated from the magnitude of signal reduction. To exclude intermolecular relaxation these experiments should be repeated at different concentrations (Liang et al., 2006). With respect to α-helical membrane proteins one spin-labeled mutant

for every transmembrane helix should be generated to obtain enough distance restraints from PRE data for structure calculations (Gottstein, Reckel, Dötsch, & Güntert, 2012).

7.2 Transmembrane Partitioning

Another interesting application of the PRE effect is the assessment of the solvent PRE for single residues of the membrane protein that is inserted into a bicelle or a nanodisc (Piai et al., 2017). [^{1}H,^{15}N]-TROSY–HSQC spectra are recorded with increasing concentration (e.g., from 0 to 20 m*M* in the case of Gd-DOTA) of a paramagnetic agent and the reduction of the peak signals is compared. If the paramagnetic agent is water-soluble and membrane impenetrable (e.g., Gd-DOTA) the signal reduction gradually decreases from the solvent-accessible parts of the membrane protein to the membrane center. Thereby, the membrane protein can be localized with respect to the center of the membrane (Piai et al., 2017) and it can provide information about membrane thickness and the membrane partitioning of a multidomain protein (Chen et al., 2018). A further prerequisite is that the bicelles or nanodiscs are of a sufficient size to prevent lateral contributions from the surrounding paramagnetic field to the relaxation (Piai et al., 2017), but most nanodiscs (Frey et al., 2017; Hagn et al., 2013; Kofuku et al., 2014) or bicelles (Laguerre et al., 2016; Morrison et al., 2012) offer this feature. In a similar fashion using spin-labeled lipids, this procedure can also be used to characterize the amino acids located within a micelle or other hydrophobic environment (Fig. 5; Sobhanifar et al., 2010).

7.3 Residual Dipolar Couplings

In general, it is beneficial to gain as much information as possible for structure calculations and therefore residual dipolar couplings could deliver additional restraints. Therefore, coupling constants under isotropic and anisotropic conditions [^{15}N^{1}H]-TROSY–HSQC and [^{15}N^{1}H]-COCAINE (Lee, Vögeli, & Pervushin, 2005) experiments are measured under unaligned and aligned conditions. As an alignment medium the bacteriophage Pf1 can be used since controls revealed no significant unspecific interaction between the discs and the phage (Bibow et al., 2014). To exclude possible interactions with a membrane protein/nanodisc or bicelle complex, the correlation times before and after addition of Pf1 should be checked by TRACT measurements (Bibow et al., 2014). If the signal overlap becomes severe, RDC measurements by HNCO experiments could be performed (Permi, Rosevear, & Annila, 2000).

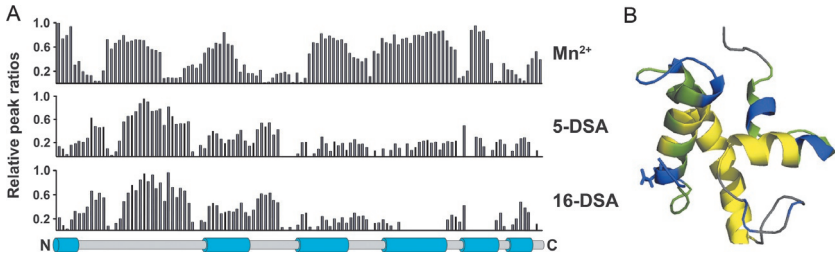

Fig. 5 Determination of protein surface accessibility by the application of paramagnetic reagents. Peak height ratios of resonances demonstrate the broadening effect by the supplementation of different paramagnetic reagents (A). Mn^{2+} indicates surface accessibility and DSA reagents identify micelle insertion. Due to the different position of the paramagnetic group at DSA, these reagents give also information about the penetration depth. The schematic representation at the bottom demonstrates the structural arrangement of CTF with helices highlighted in *blue*. In (B) the information about surface accessibility is mapped onto the CTF structure where *blue* indicates surface accessibility, *green* partially accessible regions, and *yellow* nonaccessible residues. *Adapted from Sobhanifar, S., Schneider, B., Lohr, F., Gottstein, D., Ikeya, T., Mlynarczyk, K., et al. (2010). Structural investigation of the C-terminal catalytic fragment of presenilin 1.* Proceedings of the National Academy of Sciences of the United States of America, 107*(21), 9644–9649.*

7.4 Lipid-NOEs

As lipids play a crucial role in connection with membrane proteins the elucidation of the lipid contact is of high interest (Saliba et al., 2015), especially when considering that detergent contact can drastically influence functionality and dynamics. For a first estimation if the protein is in direct contact with lipids or detergent molecules in the desired condition [^{1}H,^{15}N]-TROSY–HSQCs of the membrane protein in different environments can be compared. For example, if the resonances of a sample in bicelles are more similar to a spectrum in nanodiscs rather then detergent, it can be assumed that the membrane protein is surrounded by lipids (Frey et al., 2017).

Another more specific methodology is the detection of specific protein–lipid NOEs. Two samples are required one with conventional, protonated lipids and one with deuterated lipids. With a 3D NOESY–[^{15}N,^{1}H]-TROSY experiment, signals are visible in the sample with protonated lipids and should disappear in the sample with deuterated lipid (Fig. 6A; Laguerre et al., 2016). Within lipid mixtures or bicelles the differentiation between the lipid and detergent species could be achieved by multiple experiments with varying deuteration of the individual compounds. Thus, the presence of lipid molecules next to the membrane protein, often called the annual lipid belt,

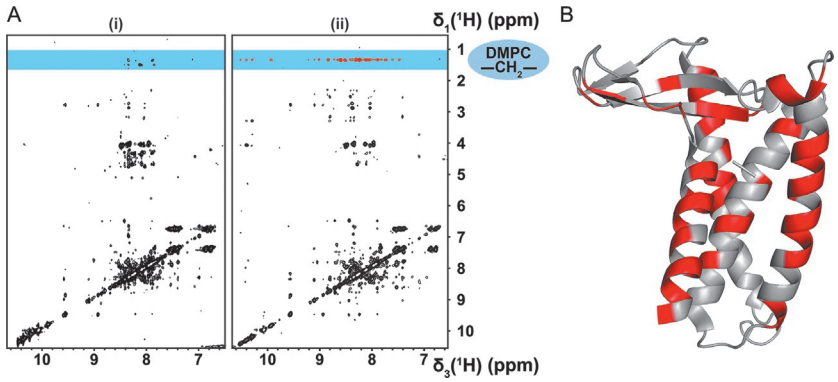

Fig. 6 Lipid-NOE measurements of LspA in bicelles after reverse q-titration. (A) NOESY–^{15}N–^{1}H-TROSY spectra of LspA. The *blue section* highlights the resonance area of the specific lipid NOEs. In (i) deuterated lipid and protonated detergent were used and in (ii) the lipid is protonated and the detergent deuterated. The residues that show NOEs to lipids are displayed in *red* on the crystal structure of LspA (PDB: 5DIR) (B). *Panel A, adapted from Laguerre, A., Löhr, F., Henrich, E., Hoffmann, B., Abdul-Manan, N., Connolly, P. J., et al. (2016). From nanodiscs to isotropic bicelles: A procedure for solution nuclear magnetic resonance studies of detergent-sensitive integral membrane proteins.* Structure, 24*(10), 1830–1841.*

can be detected and lipid contact sites can be mapped (Fig. 6B; Laguerre et al., 2016). Here, also information about the membrane partitioning can be extracted by assigning the residues presenting lipid NOEs (Chen et al., 2018). This technique can also be used for verifying specific interactions of the membrane protein with a certain lipid on a certain position (Zhao, Wang, Run, OuYang, & Chou, 2016). Since the chemical environment of methylene groups in acyl chain moieties of different lipids or detergents is quite similar, multiple samples with differential deuteration of the individual components are required as well.

8. OUTLOOK

With perspectives of EM resolution revolution or in meso crystallization the role for NMR in structure determination of membrane proteins becomes smaller. On the other hand, solution NMR is the method of choice to address questions of protein dynamics in solution (Liang & Tamm, 2016; Palmer, 2004), which is problematic with static techniques. Taken into account that the role of lipids for membrane proteins with respect to complex integrity (Gupta et al., 2017; Henrich et al., 2017), modulation of

dynamics (Martens et al., 2016), or regulation (Cong, Liu, Liu, Liang, & Laganowsky, 2017) gets into the focus of current research, it is beneficial that bilayer environments like nanodiscs or bicelles become compatible with solution-state NMR. By detecting the overall characteristics in bilayers or distinct interactions with lipids by, for example, protein–lipid NOEs, NMR provides manifold opportunities for the analysis of membrane proteins. Here, the combination with other techniques such as native mass spectrometry (Barrera & Robinson, 2011) could be highly beneficial for the identification of the interplay with specific lipids. As lipid mixtures get more and more popular the differentiation between different lipid species could be achieved by directed delipidation strategies (Bechara et al., 2015).

The problematic increase in sample particle size when using bilayer environments for solution NMR will be addressed in future by continuously probing new hydrophobic environments. Already for a few years nanodiscs based on chemical polymers (SMALPs) are evaluated especially for solid-state NMR (Bersch, Dörr, Hessel, Killian, & Schanda, 2017; Orwick-Rydmark et al., 2012), but due to their low pH and salt tolerance as well as their still large size not applicable to solution NMR so far. However, the continuous modification of the polymers probably will enable their use in the future in solution NMR as well (Fiori, Jiang, Altenberg, & Liang, 2017; Ravula, Ramadugu, Di Mauro, & Ramamoorthy, 2017). For enhanced spectral resolution of membrane proteins inserted into nanodiscs the Wagner lab recently proposed an approach to covalently circulate the MSP scaffold protein, thus limiting the size variation of resulting nanodiscs (Nasr et al., 2017). Alternative nanodisc-like environments having a scaffold not based on Apo-A1 derivatives but on the lipid-binding protein saposin emerged recently (Frauenfeld et al., 2016). The advantage of such salipro particles is the increased flexibility in adjusting their size according to the dimension of the inserted membrane protein, while the required amount of lipids to solubilize the membrane protein is kept at a minimum. This reduces the overall size of the particle and their entry into solution-state NMR experiments is currently emerging (Chien et al., 2017).

Further improvements are expected in methods and costs for stable isotope labeling. Cell-free expression is already an efficient platform for the production of specifically labeled samples also due to the reduced scrambling (LaGuerre et al., 2015). With the recently gained information on the lysate proteome (Foshag et al., 2018), it is now possible to directly use and optimize residual metabolic pathways for the generation of specifically labeled amino acids (Lazarova et al., 2018). Also the efficient incorporation of

nonnatural amino acids (Jones et al., 2010) with NMR active isotopes (Manglik et al., 2015) becomes feasible with cell-free expression approaches (Martin et al., 2018; Peuker et al., 2016).

ACKNOWLEDGMENTS

This work was funded by the Collaborative Research Center (SFB) 807 of the German Research Foundation (DFG), the Center for Biomolecular Magnetic Resonance (BMRZ) by the state of Hessen, and the Cluster of Excellence in Frankfurt (Macromolecular Complexes).

REFERENCES

Amero, C., Schanda, P., Durá, M. A., Ayala, I., Marion, D., Franzetti, B., et al. (2009). Fast two-dimensional NMR spectroscopy of high molecular weight protein assemblies. *Journal of the American Chemical Society*, *131*(10), 3448–3449.

Barna, J. C. J., & Laue, E. D. (1987). Conventional and exponential sampling for 2D NMR experiments with application to a 2D NMR spectrum of a protein. *Journal of Magnetic Resonance (1969)*, *75*(2), 384–389.

Barrera, N. P., & Robinson, C. V. (2011). Advances in the mass spectrometry of membrane proteins: From individual proteins to intact complexes. *Annual Review of Biochemistry*, *80*, 247–271.

Barrera, N. P., Zhou, M., & Robinson, C. V. (2013). The role of lipids in defining membrane protein interactions: Insights from mass spectrometry. *Trends in Cell Biology*, *23*(1), 1–8.

Bax, A., & Ikura, M. (1991). An efficient 3D NMR technique for correlating the proton and 15N backbone amide resonances with the alpha-carbon of the preceding residue in uniformly 15N/13C enriched proteins. *Journal of Biomolecular NMR*, *1*(1), 99–104.

Bayburt, T. H., Grinkova, Y. V., & Sligar, S. G. (2002). Self-assembly of discoidal phospholipid bilayer nanoparticles with membrane scaffold proteins. *Nano Letters*, *2*(8), 853–856.

Bayburt, T. H., & Sligar, S. G. (2003). Self-assembly of single integral membrane proteins into soluble nanoscale phospholipid bilayers. *Protein Science*, *12*(11), 2476–2481.

Bechara, C., Nöll, A., Morgner, N., Degiacomi, M. T., Tampé, R., & Robinson, C. V. (2015). A subset of annular lipids is linked to the flippase activity of an ABC transporter. *Nature Chemistry*, *7*(3), 255–262.

Bersch, B., Dörr, J. M., Hessel, A., Killian, J. A., & Schanda, P. (2017). Proton-detected solid-state NMR spectroscopy of a zinc diffusion facilitator protein in native nanodiscs. *Angewandte Chemie (International Ed. in English)*, *56*(9), 2508–2512.

Bibow, S., Carneiro, M. G., Sabo, T. M., Schwiegk, C., Becker, S., Riek, R., et al. (2014). Measuring membrane protein bond orientations in nanodiscs via residual dipolar couplings. *Protein Science*, *23*(7), 851–856.

Caffrey, M. (2015). A comprehensive review of the lipid cubic phase or in meso method for crystallizing membrane and soluble proteins and complexes. *Acta Crystallographica. Section F, Structural Biology Communications*, *71*(Pt. 1), 3–18.

Chen, W., Dev, J., Mezhyrova, J., Pan, L., Piai, A., & Chou, J. J. (2018). The unusual transmembrane partition of the hexameric channel of the hepatitis C virus. *Structure*, *26*(4), 627–634.e624.

Chien, C. H., Helfinger, L. R., Bostock, M. J., Solt, A., Tan, Y. L., & Nietlispach, D. (2017). An adaptable phospholipid membrane mimetic system for solution NMR studies of membrane proteins. *Journal of the American Chemical Society*, *139*(42), 14829–14832.

Clore, G. M., Kay, L. E., Bax, A., & Gronenborn, A. M. (1991). Four-dimensional 13C/13C-edited nuclear Overhauser enhancement spectroscopy of a protein in solution: Application to interleukin 1 beta. *Biochemistry*, *30*(1), 12–18.

Clubb, A. T., Thanabal, V., & Wagner, G. (1992). A constant-time three-dimensional triple-resonance pulse scheme to correlate intraresidue ^{1}H, ^{15}N, $^{13}C'$ chemical shifts in ^{15}N-^{13}C-labeled proteins. *Journal of Magnetic Resonance*, *97*, 213–217.

Cong, X., Liu, Y., Liu, W., Liang, X., & Laganowsky, A. (2017). Allosteric modulation of protein-protein interactions by individual lipid binding events. *Nature Communications*, *8*(1), 2203.

Davis, A. L., Laue, E. D., & Keeler, J. (1991). Absorption-mode two-dimensional NMR spectra recorded using pulsed field gradients. *Journal of Magnetic Resonance (1969)*, *94*(3), 637–644.

Dawaliby, R., Trubbia, C., Delporte, C., Masureel, M., Van Antwerpen, P., Kobilka, B. K., et al. (2016). Allosteric regulation of G protein-coupled receptor activity by phospholipids. *Nature Chemical Biology*, *12*(1), 35–39.

Dehez, F., Schanda, P., King, M. S., Kunji, E. R. S., & Chipot, C. (2017). Mitochondrial ADP/ATP carrier in dodecylphosphocholine binds cardiolipins with non-native affinity. *Biophysical Journal*, *113*(11), 2311–2315.

Denisov, I. G., Grinkova, Y. V., Lazarides, A. A., & Sligar, S. G. (2004). Directed self-assembly of monodisperse phospholipid bilayer nanodiscs with controlled size. *Journal of the American Chemical Society*, *126*(11), 3477–3487.

Denisov, I. G., & Sligar, S. G. (2016). Nanodiscs for structural and functional studies of membrane proteins. *Nature Structural & Molecular Biology*, *23*(6), 481–486.

Denisov, I. G., & Sligar, S. G. (2017). Nanodiscs in membrane biochemistry and biophysics. *Chemical Reviews*, *117*(6), 4669–4713.

Dötsch, V., Oswald, R. E., & Wagner, G. (1996). Amino-acid-type-selective triple-resonance experiments. *Journal of Magnetic Resonance. Series B*, *110*(1), 107–111.

Dürr, U. H., Gildenberg, M., & Ramamoorthy, A. (2012). The magic of bicelles lights up membrane protein structure. *Chemical Reviews*, *112*(11), 6054–6074.

Efremov, R. G., Gatsogiannis, C., & Raunser, S. (2017). Lipid nanodiscs as a tool for high-resolution structure determination of membrane proteins by single-particle cryo-EM. *Methods in Enzymology*, *594*, 1–30.

Etzkorn, M., Raschle, T., Hagn, F., Gelev, V., Rice, A. J., Walz, T., et al. (2013). Cell-free expressed bacteriorhodopsin in different soluble membrane mimetics: Biophysical properties and NMR accessibility. *Structure*, *21*(3), 394–401.

Feuerstein, S., Plevin, M. J., Willbold, D., & Brutscher, B. (2012). iHADAMAC: A complementary tool for sequential resonance assignment of globular and highly disordered proteins. *Journal of Magnetic Resonance*, *214*(1), 329–334.

Fiori, M. C., Jiang, Y., Altenberg, G. A., & Liang, H. (2017). Polymer-encased nanodiscs with improved buffer compatibility. *Scientific Reports*, *7*(1), 7432.

Foshag, D., Henrich, E., Hiller, E., Schäfer, M., Kerger, C., Burger-Kentischer, A., et al. (2018). The E. coli S30 lysate proteome: A prototype for cell-free protein production. *New Biotechnology*, *40*(Pt. B), 245–260.

Frauenfeld, J., Löving, R., Armache, J. P., Sonnen, A. F., Guettou, F., Moberg, P., et al. (2016). A saposin-lipoprotein nanoparticle system for membrane proteins. *Nature Methods*, *13*(4), 345–351.

Frenkiel, T., Bauer, C., Carr, M. D., Birdsall, B., & Feeney, J. (1990). HMQC-NOESY-HMQC, a three-dimensional NMR experiment which allows detection of nuclear overhauser effects between protons with overlapping signals. *Journal of Magnetic Resonance (1969)*, *90*(2), 420–425.

Frey, L., Lakomek, N. A., Riek, R., & Bibow, S. (2017). Micelles, bicelles, and nanodiscs: Comparing the impact of membrane mimetics on membrane protein backbone dynamics. *Angewandte Chemie (International Ed. in English)*, *56*(1), 380–383.

Gardner, K. H., & Kay, L. E. (1997). Production and incorporation of 15N, 13C, 2H (1H-δ1 methyl) isoleucine into proteins for multidimensional NMR studies. *Journal of the American Chemical Society*, *119*(32), 7599–7600.

Glück, J. M., Wittlich, M., Feuerstein, S., Hoffmann, S., Willbold, D., & Koenig, B. W. (2009). Integral membrane proteins in nanodiscs can be studied by solution NMR spectroscopy. *Journal of the American Chemical Society*, *131*(34), 12060–12061.

Goto, N. K., Gardner, K. H., Mueller, G. A., Willis, R. C., & Kay, L. E. (1999). A robust and cost-effective method for the production of Val, Leu, Ile (delta 1) methyl-protonated 15N-, 13C-, 2H-labeled proteins. *Journal of Biomolecular NMR*, *13*(4), 369–374.

Gottstein, D., Reckel, S., Dötsch, V., & Güntert, P. (2012). Requirements on paramagnetic relaxation enhancement data for membrane protein structure determination by NMR. *Structure*, *20*(6), 1019–1027.

Griffey, R. H., Redfield, A. G., Loomis, R. E., & Dahlquist, F. W. (1985). Nuclear magnetic resonance observation and dynamics of specific amide protons in T4 lysozyme. *Biochemistry*, *24*(4), 817–822.

Griffey, R. H., Redfield, A. G., McIntosh, L. P., Oas, T. G., & Dahlquist, F. W. (1986). Assignment of proton amide resonances of T4 lysozyme by carbon-13 and nitrogen-15 multiple isotopic labeling. *Journal of the American Chemical Society*, *108*(21), 6816–6817.

Guignard, L., Ozawa, K., Pursglove, S. E., Otting, G., & Dixon, N. E. (2002). NMR analysis of in vitro-synthesized proteins without purification: A high-throughput approach. *FEBS Letters*, *524*(1–3), 159–162.

Gupta, K., Donlan, J. A. C., Hopper, J. T. S., Uzdavinys, P., Landreh, M., Struwe, W. B., et al. (2017). The role of interfacial lipids in stabilizing membrane protein oligomers. *Nature*, *541*(7637), 421–424.

Hagn, F., Etzkorn, M., Raschle, T., & Wagner, G. (2013). Optimized phospholipid bilayer nanodiscs facilitate high-resolution structure determination of membrane proteins. *Journal of the American Chemical Society*, *135*(5), 1919–1925.

Hagn, F., & Wagner, G. (2015). Structure refinement and membrane positioning of selectively labeled OmpX in phospholipid nanodiscs. *Journal of Biomolecular NMR*, *61*(3–4), 249–260.

Harbers, M. (2014). Wheat germ systems for cell-free protein expression. *FEBS Letters*, *588*(17), 2762–2773.

Harris, N. J., Reading, E., Ataka, K., Grzegorzewski, L., Charalambous, K., Liu, X., et al. (2017). Structure formation during translocon-unassisted co-translational membrane protein folding. *Scientific Reports*, *7*(1), 8021.

He, Y., Wang, K., & Yan, N. (2014). The recombinant expression systems for structure determination of eukaryotic membrane proteins. *Protein & Cell*, *5*(9), 658–672.

Hefke, F., Bagaria, A., Reckel, S., Ullrich, S. J., Dötsch, V., Glaubitz, C., et al. (2011). Optimization of amino acid type-specific 13C and 15N labeling for the backbone assignment of membrane proteins by solution- and solid-state NMR with the UPLABEL algorithm. *Journal of Biomolecular NMR*, *49*(2), 75–84.

Hein, C., Löhr, F., Schwarz, D., & Dötsch, V. (2017). Acceleration of protein backbone NMR assignment by combinatorial labeling: Application to a small molecule binding study. *Biopolymers*, *107*(5), e23013.

Henrich, E., Dötsch, V., & Bernhard, F. (2015). Screening for lipid requirements of membrane proteins by combining cell-free expression with nanodiscs. *Methods in Enzymology*, *556*, 351–369.

Henrich, E., Hein, C., Dötsch, V., & Bernhard, F. (2015). Membrane protein production in Escherichia coli cell-free lysates. *FEBS Letters*, *589*(15), 1713–1722.

Henrich, E., Ma, Y., Engels, I., Münch, D., Otten, C., Schneider, T., et al. (2016). Lipid requirements for the enzymatic activity of MraY translocases and in vitro reconstitution of the lipid II synthesis pathway. *The Journal of Biological Chemistry*, *291*(5), 2535–2546.

Henrich, E., Peetz, O., Hein, C., Laguerre, A., Hoffmann, B., Hoffmann, J., et al. (2017). Analyzing native membrane protein assembly in nanodiscs by combined non-covalent mass spectrometry and synthetic biology. *eLife*, *6*(6), e20954.

Hiller, S., Ibraghimov, I., Wagner, G., & Orekhov, V. Y. (2009). Coupled decomposition of four-dimensional NOESY spectra. *Journal of the American Chemical Society*, *131*(36), 12970–12978.

Hoffmann, B., Löhr, F., Laguerre, A., Bernhard, F., & Dötsch, V. (2018). Protein labeling strategies for liquid-state NMR spectroscopy using cell-free synthesis. *Progress in Nuclear Magnetic Resonance Spectroscopy*, *105*, 1–22.

Holland, D. J., Bostock, M. J., Gladden, L. F., & Nietlispach, D. (2011). Fast multi-dimensional NMR spectroscopy using compressed sensing. *Angewandte Chemie (International Ed. in English)*, *50*(29), 6548–6551.

Hong, S. H., Ntai, I., Haimovich, A. D., Kelleher, N. L., Isaacs, F. J., & Jewett, M. C. (2014). Cell-free protein synthesis from a release factor 1 deficient Escherichia coli activates efficient and multiple site-specific nonstandard amino acid incorporation. *ACS Synthetic Biology*, *3*(6), 398–409.

Hurst, G. B., Asano, K. G., Doktycz, C. J., Consoli, E. J., Doktycz, W. L., Foster, C. M., et al. (2017). Proteomics-based tools for evaluation of cell-free protein synthesis. *Analytical Chemistry*, *89*(21), 11443–11451.

Ikura, M., Kay, L. E., & Bax, A. (1990). A novel approach for sequential assignment of 1H, 13C, and 15N spectra of proteins: Heteronuclear triple-resonance three-dimensional NMR spectroscopy. Application to calmodulin. *Biochemistry*, *29*(19), 4659–4667.

Ikura, M., Krinks, M., Torchia, D. A., & Bax, A. (1990). An efficient NMR approach for obtaining sequence-specific resonance assignments of larger proteins based on multiple isotopic labeling. *FEBS Letters*, *266*(1–2), 155–158.

Ilgü, H., Jeckelmann, J. M., Gachet, M. S., Boggavarapu, R., Ucurum, Z., Gertsch, J., et al. (2014). Variation of the detergent-binding capacity and phospholipid content of membrane proteins when purified in different detergents. *Biophysical Journal*, *106*(8), 1660–1670.

Isogai, S., Deupi, X., Opitz, C., Heydenreich, F. M., Tsai, C. J., Brueckner, F., et al. (2016). Backbone NMR reveals allosteric signal transduction networks in the β1-adrenergic receptor. *Nature*, *530*(7589), 237–241.

Jaipuria, G., Krishnarjuna, B., Mondal, S., Dubey, A., & Atreya, H. S. (2012). Amino acid selective labeling and unlabeling for protein resonance assignments. *Advances in Experimental Medicine and Biology*, *992*, 95–118.

Jones, D. H., Cellitti, S. E., Hao, X., Zhang, Q., Jahnz, M., Summerer, D., et al. (2010). Site-specific labeling of proteins with NMR-active unnatural amino acids. *Journal of Biomolecular NMR*, *46*(1), 89–100.

Kainosho, M., & Tsuji, T. (1982). Assignment of the three methionyl carbonyl carbon resonances in Streptomyces subtilisin inhibitor by a carbon-13 and nitrogen-15 double-labeling technique. A new strategy for structural studies of proteins in solution. *Biochemistry*, *21*(24), 6273–6279.

Kasai, T., Koshiba, S., Yokoyama, J., & Kigawa, T. (2015). Stable isotope labeling strategy based on coding theory. *Journal of Biomolecular NMR*, *63*(2), 213–221.

Kato, K., Matsunaga, C., Nishimura, Y., Waelchli, M., Kainosho, M., & Arata, Y. (1989). Application of 13C nuclear magnetic resonance spectroscopy to molecular structural analyses of antibody molecules. *Journal of Biochemistry*, *105*(6), 867–869.

Katzen, F., Fletcher, J. E., Yang, J. P., Kang, D., Peterson, T. C., Cappuccio, J. A., et al. (2008). Insertion of membrane proteins into discoidal membranes using a cell-free protein expression approach. *Journal of Proteome Research*, *7*(8), 3535–3542.

Kay, L. E., Clore, G. M., Bax, A., & Gronenborn, A. M. (1990). Four-dimensional heteronuclear triple-resonance NMR spectroscopy of interleukin-1 beta in solution. *Science*, *249*(4967), 411–414.

Kigawa, T., Yabuki, T., Matsuda, N., Matsuda, T., Nakajima, R., Tanaka, A., et al. (2004). Preparation of Escherichia coli cell extract for highly productive cell-free protein expression. *Journal of Structural and Functional Genomics*, *5*(1–2), 63–68.

Kim, H. J., Howell, S. C., Van Horn, W. D., Jeon, Y. H., & Sanders, C. R. (2009). Recent advances in the application of solution NMR spectroscopy to multi-span integral membrane proteins. *Progress in Nuclear Magnetic Resonance Spectroscopy*, *55*(4), 335–360.

Kim, T. W., Keum, J. W., Oh, I. S., Choi, C. Y., Park, C. G., & Kim, D. M. (2006). Simple procedures for the construction of a robust and cost-effective cell-free protein synthesis system. *Journal of Biotechnology*, *126*(4), 554–561.

Kim, J., Wu, S., Tomasiak, T. M., Mergel, C., Winter, M. B., Stiller, S. B., et al. (2015). Subnanometre-resolution electron cryomicroscopy structure of a heterodimeric ABC exporter. *Nature*, *517*(7534), 396–400.

Klammt, C., Löhr, F., Schäfer, B., Haase, W., Dötsch, V., Rüterjans, H., et al. (2004). High level cell-free expression and specific labeling of integral membrane proteins. *European Journal of Biochemistry*, *271*(3), 568–580.

Kofuku, Y., Ueda, T., Okude, J., Shiraishi, Y., Kondo, K., Maeda, M., et al. (2012). Efficacy of the β2-adrenergic receptor is determined by conformational equilibrium in the transmembrane region. *Nature Communications*, *3*, 1045.

Kofuku, Y., Ueda, T., Okude, J., Shiraishi, Y., Kondo, K., Mizumura, T., et al. (2014). Functional dynamics of deuterated β2-adrenergic receptor in lipid bilayers revealed by NMR spectroscopy. *Angewandte Chemie (International Ed. in English)*, *53*(49), 13376–13379.

Kühlbrandt, W. (2014). The resolution revolution. *Science*, *343*(6178), 1443–1444.

Kurauskas, V., Hessel, A., Ma, P., Lunetti, P., Weinhäupl, K., Imbert, L., et al. (2018). How detergent impacts membrane proteins: Atomic-level views of mitochondrial carriers in dodecylphosphocholine. *Journal of Physical Chemistry Letters*, *9*(5), 933–938.

Kwon, Y. C., & Jewett, M. C. (2015). High-throughput preparation methods of crude extract for robust cell-free protein synthesis. *Scientific Reports*, *5*, 8663.

LaGuerre, A., Löhr, F., Bernhard, F., & Dötsch, V. (2015). Labeling of membrane proteins by cell-free expression. *Methods in Enzymology*, *565*, 367–388.

Laguerre, A., Löhr, F., Henrich, E., Hoffmann, B., Abdul-Manan, N., Connolly, P. J., et al. (2016). From nanodiscs to isotropic bicelles: A procedure for solution nuclear magnetic resonance studies of detergent-sensitive integral membrane proteins. *Structure*, *24*(10), 1830–1841.

Lazarova, M., Lőhr, F., Rues, R. B., Kleebach, R., Dötsch, V., & Bernhard, F. (2018). Precursor-based selective methyl labelling of cell-free synthesized proteins. *ACS Chemical Biology*, *13*(8), 2170–2178. https://doi.org/10.1021/acschembio.8b00338.

Lee, D., Hilty, C., Wider, G., & Wüthrich, K. (2006). Effective rotational correlation times of proteins from NMR relaxation interference. *Journal of Magnetic Resonance*, *178*(1), 72–76.

Lee, D., Vögeli, B., & Pervushin, K. (2005). Detection of C′,Calpha correlations in proteins using a new time- and sensitivity-optimal experiment. *Journal of Biomolecular NMR*, *31*(4), 273–278.

LeMaster, D. M., & Richards, F. M. (1985). 1H-15N heteronuclear NMR studies of Escherichia coli thioredoxin in samples isotopically labeled by residue type. *Biochemistry*, *24*(25), 7263–7268.

Li, Y., Kijac, A. Z., Sligar, S. G., & Rienstra, C. M. (2006). Structural analysis of nanoscale self-assembled discoidal lipid bilayers by solid-state NMR spectroscopy. *Biophysical Journal*, *91*(10), 3819–3828.

Liang, B., Bushweller, J. H., & Tamm, L. K. (2006). Site-directed parallel spin-labeling and paramagnetic relaxation enhancement in structure determination of membrane proteins by solution NMR spectroscopy. *Journal of the American Chemical Society*, *128*(13), 4389–4397.

Liang, B., & Tamm, L. K. (2016). NMR as a tool to investigate the structure, dynamics and function of membrane proteins. *Nature Structural & Molecular Biology*, *23*(6), 468–474.

Lichtenecker, R. J., Coudevylle, N., Konrat, R., & Schmid, W. (2013). Selective isotope labelling of leucine residues by using α-ketoacid precursor compounds. *Chembiochem*, *14*(7), 818–821.

Löhr, F., Laguerre, A., Bock, C., Reckel, S., Connolly, P. J., Abdul-Manan, N., et al. (2014). Time-shared experiments for efficient assignment of triple-selectively labeled proteins. *Journal of Magnetic Resonance*, *248*, 81–95.

Löhr, F., Reckel, S., Karbyshev, M., Connolly, P. J., Abdul-Manan, N., Bernhard, F., et al. (2012). Combinatorial triple-selective labeling as a tool to assist membrane protein backbone resonance assignment. *Journal of Biomolecular NMR*, *52*(3), 197–210.

Löhr, F., Tumulka, F., Bock, C., Abele, R., & Dötsch, V. (2015). An extended combinatorial 15N, 13Cα, and 13C' labeling approach to protein backbone resonance assignment. *Journal of Biomolecular NMR*, *62*(3), 263–279.

Luan, T., Jaravine, V., Yee, A., Arrowsmith, C. H., & Orekhov, V. Y. (2005). Optimization of resolution and sensitivity of 4D NOESY using multi-dimensional decomposition. *Journal of Biomolecular NMR*, *33*(1), 1–14.

Lyukmanova, E. N., Shenkarev, Z. O., Khabibullina, N. F., Kopeina, G. S., Shulepko, M. A., Paramonov, A. S., et al. (2012). Lipid-protein nanodiscs for cell-free production of integral membrane proteins in a soluble and folded state: Comparison with detergent micelles, bicelles and liposomes. *Biochimica et Biophysica Acta*, *1818*(3), 349–358.

Madin, K., Sawasaki, T., Ogasawara, T., & Endo, Y. (2000). A highly efficient and robust cell-free protein synthesis system prepared from wheat embryos: Plants apparently contain a suicide system directed at ribosomes. *Proceedings of the National Academy of Sciences of the United States of America*, *97*(2), 559–564.

Manglik, A., Kim, T. H., Masureel, M., Altenbach, C., Yang, Z., Hilger, D., et al. (2015). Structural insights into the dynamic process of β2-adrenergic receptor signaling. *Cell*, *161*(5), 1101–1111.

Martens, C., Stein, R. A., Masureel, M., Roth, A., Mishra, S., Dawaliby, R., et al. (2016). Lipids modulate the conformational dynamics of a secondary multidrug transporter. *Nature Structural & Molecular Biology*, *23*(8), 744–751.

Martin, R. W., Des Soye, B. J., Kwon, Y. C., Kay, J., Davis, R. G., Thomas, P. M., et al. (2018). Cell-free protein synthesis from genomically recoded bacteria enables multisite incorporation of noncanonical amino acids. *Nature Communications*, *9*(1), 1203.

Marty, M. T., Wilcox, K. C., Klein, W. L., & Sligar, S. G. (2013). Nanodisc-solubilized membrane protein library reflects the membrane proteome. *Analytical and Bioanalytical Chemistry*, *405*(12), 4009–4016.

Maslennikov, I., & Choe, S. (2013). Advances in NMR structures of integral membrane proteins. *Current Opinion in Structural Biology*, *23*(4), 555–562.

Maslennikov, I., Klammt, C., Hwang, E., Kefala, G., Okamura, M., Esquivies, L., et al. (2010). Membrane domain structures of three classes of histidine kinase receptors by cell-free expression and rapid NMR analysis. *Proceedings of the National Academy of Sciences of the United States of America*, *107*(24), 10902–10907.

McClary, W. D., Sumida, J. P., Scian, M., Paço, L., & Atkins, W. M. (2016). Membrane fluidity modulates thermal stability and ligand binding of cytochrome P4503A4 in lipid nanodiscs. *Biochemistry*, *55*(45), 6258–6268.

Miyanoiri, Y., Takeda, M., Okuma, K., Ono, A. M., Terauchi, T., & Kainosho, M. (2013). Differential isotope-labeling for Leu and Val residues in a protein by E. coli cellular expression using stereo-specifically methyl labeled amino acids. *Journal of Biomolecular NMR*, *57*(3), 237–249.

Mobli, M., & Hoch, J. C. (2014). Nonuniform sampling and non-Fourier signal processing methods in multidimensional NMR. *Progress in Nuclear Magnetic Resonance Spectroscopy*, *83*, 21–41.

Morrison, E. A., DeKoster, G. T., Dutta, S., Vafabakhsh, R., Clarkson, M. W., Bahl, A., et al. (2012). Antiparallel EmrE exports drugs by exchanging between asymmetric structures. *Nature*, *481*(7379), 45–50.

Muchmore, D. C., McIntosh, L. P., Russell, C. B., Anderson, D. E., & Dahlquist, F. W. (1989). Expression and nitrogen-15 labeling of proteins for proton and nitrogen-15 nuclear magnetic resonance. *Methods in Enzymology*, *177*, 44–73.

Nasr, M. L., Baptista, D., Strauss, M., Sun, Z. J., Grigoriu, S., Huser, S., et al. (2017). Covalently circularized nanodiscs for studying membrane proteins and viral entry. *Nature Methods*, *14*(1), 49–52.

Nikolaev, M., Round, E., Gushchin, I., Polovinkin, V., Balandin, T., Kuzmichev, P., et al. (2017). Integral membrane proteins can be crystallized directly from nanodiscs. *Crystal Growth & Design*, *17*(3), 945–948.

Nygaard, R., Zou, Y., Dror, R. O., Mildorf, T. J., Arlow, D. H., Manglik, A., et al. (2013). The dynamic process of β(2)-adrenergic receptor activation. *Cell*, *152*(3), 532–542.

Ollerenshaw, J. E., Tugarinov, V., & Kay, L. E. (2003). Methyl TROSY: Explanation and experimental verification. *Magnetic Resonance in Chemistry*, *41*(10), 843–852.

Orekhov, V. Y., Ibraghimov, I., & Billeter, M. (2003). Optimizing resolution in multidimensional NMR by three-way decomposition. *Journal of Biomolecular NMR*, *27*(2), 165–173.

Orekhov, V. Y., & Jaravine, V. A. (2011). Analysis of non-uniformly sampled spectra with multi-dimensional decomposition. *Progress in Nuclear Magnetic Resonance Spectroscopy*, *59*(3), 271–292.

Orwick-Rydmark, M., Lovett, J. E., Graziadei, A., Lindholm, L., Hicks, M. R., & Watts, A. (2012). Detergent-free incorporation of a seven-transmembrane receptor protein into nanosized bilayer Lipodisq particles for functional and biophysical studies. *Nano Letters*, *12*(9), 4687–4692.

Palmer, A. G. (2004). NMR characterization of the dynamics of biomacromolecules. *Chemical Reviews*, *104*(8), 3623–3640.

Pantoja-Uceda, D., & Santoro, J. (2008). Amino acid type identification in NMR spectra of proteins via beta- and gamma-carbon edited experiments. *Journal of Magnetic Resonance*, *195*(2), 187–195.

Parker, M. J., Aulton-Jones, M., Hounslow, A. M., & Craven, C. J. (2004). A combinatorial selective labeling method for the assignment of backbone amide NMR resonances. *Journal of the American Chemical Society*, *126*(16), 5020–5021.

Peetz, O., Henrich, E., Laguerre, A., Löhr, F., Hein, C., Dötsch, V., et al. (2017). Insights into cotranslational membrane protein insertion by combined LILBID-mass spectrometry and NMR spectroscopy. *Analytical Chemistry*, *89*(22), 12314–12318.

Permi, P., Rosevear, P. R., & Annila, A. (2000). A set of HNCO-based experiments for measurement of residual dipolar couplings in 15N, 13C, (2H)-labeled proteins. *Journal of Biomolecular NMR*, *17*(1), 43–54.

Pervushin, K., Riek, R., Wider, G., & Wüthrich, K. (1997). Attenuated T2 relaxation by mutual cancellation of dipole-dipole coupling and chemical shift anisotropy indicates an avenue to NMR structures of very large biological macromolecules in solution. *Proceedings of the National Academy of Sciences of the United States of America*, *94*(23), 12366–12371.

Peuker, S., Andersson, H., Gustavsson, E., Maiti, K. S., Kania, R., Karim, A., et al. (2016). Efficient isotope editing of proteins for site-directed vibrational spectroscopy. *Journal of the American Chemical Society*, *138*(7), 2312–2318.

Piai, A., Fu, Q., Dev, J., & Chou, J. J. (2017). Optimal bicelle size q for solution NMR studies of the protein transmembrane partition. *Chemistry*, *23*(6), 1361–1367.

Rasmussen, S. G., Choi, H. J., Fung, J. J., Pardon, E., Casarosa, P., Chae, P. S., et al. (2011). Structure of a nanobody-stabilized active state of the beta(2) adrenoceptor. *Nature*, *469*(7329), 175–180.

Rasmussen, S. G., Choi, H. J., Rosenbaum, D. M., Kobilka, T. S., Thian, F. S., Edwards, P. C., et al. (2007). Crystal structure of the human beta2 adrenergic G-protein-coupled receptor. *Nature*, *450*(7168), 383–387.

Ravula, T., Ramadugu, S. K., Di Mauro, G., & Ramamoorthy, A. (2017). Bioinspired, size-tunable self-assembly of polymer-lipid bilayer nanodiscs. *Angewandte Chemie (International Ed. in English)*, *56*(38), 11466–11470.

Reckel, S., Gottstein, D., Stehle, J., Löhr, F., Verhoefen, M. K., Takeda, M., et al. (2011). Solution NMR structure of proteorhodopsin. *Angewandte Chemie (International Ed. in English)*, *50*(50), 11942–11946.

Reckel, S., Sobhanifar, S., Durst, F., Lohr, F., Shirokov, V. A., Dötsch, V., et al. (2010). Strategies for the cell-free expression of membrane proteins. *Methods in Molecular Biology*, *607*, 187–212.

Reckel, S., Sobhanifar, S., Schneider, B., Junge, F., Schwarz, D., Durst, F., et al. (2008). Transmembrane segment enhanced labeling as a tool for the backbone assignment of alpha-helical membrane proteins. *Proceedings of the National Academy of Sciences of the United States of America*, *105*(24), 8262–8267.

Riek, R., Wider, G., Pervushin, K., & Wüthrich, K. (1999). Polarization transfer by cross-correlated relaxation in solution NMR with very large molecules. *Proceedings of the National Academy of Sciences of the United States of America*, *96*(9), 4918–4923.

Roos, C., Kai, L., Haberstock, S., Proverbio, D., Ghoshdastider, U., Ma, Y., et al. (2014). High-level cell-free production of membrane proteins with nanodiscs. *Methods in Molecular Biology*, *1118*, 109–130.

Roos, C., Zocher, M., Müller, D., Münch, D., Schneider, T., Sahl, H. G., et al. (2012). Characterization of co-translationally formed nanodisc complexes with small multidrug transporters, proteorhodopsin and with the E. coli MraY translocase. *Biochimica et Biophysica Acta*, *1818*(12), 3098–3106.

Rossi, P., Xia, Y., Khanra, N., Veglia, G., & Kalodimos, C. G. (2016). ^{15}N and ^{13}C-SOFAST-HMQC editing enhances 3D-NOESY sensitivity in highly deuterated, selectively [^{1}H,^{13}C]-labeled proteins. *Journal of Biomolecular NMR*, *66*(4), 259–271.

Rovnyak, D., Hoch, J. C., Stern, A. S., & Wagner, G. (2004). Resolution and sensitivity of high field nuclear magnetic resonance spectroscopy. *Journal of Biomolecular NMR*, *30*(1), 1–10.

Rues, R. B., Dong, F., Dötsch, V., & Bernhard, F. (2018). Systematic optimization of cell-free synthesized human endothelin B receptor folding. *Methods*, *147*, 73–83. https://doi.org/10.1016/j.ymeth.2018.01.012.

Rues, R. B., Dötsch, V., & Bernhard, F. (2016). Co-translational formation and pharmacological characterization of beta1-adrenergic receptor/nanodisc complexes with different lipid environments. *Biochimica et Biophysica Acta*, *1858*(6), 1306–1316.

Rule, G. S., Tjandra, N., Simplaceanu, V., & Ho, C. (1993). Assignment strategies for ^{15}N-^{1}H correlated spectra of large proteins in solution. *Journal of Magnetic Resonance. Series B*, *102*, 126–128.

Saliba, A. E., Vonkova, I., & Gavin, A. C. (2015). The systematic analysis of protein-lipid interactions comes of age. *Nature Reviews. Molecular Cell Biology*, *16*(12), 753–761.

Sanders, C. R., & Sönnichsen, F. (2006). Solution NMR of membrane proteins: Practice and challenges. *Magnetic Resonance in Chemistry: MRC*, *44*, S24–S40. Spec. No.

Schanda, P., & Brutscher, B. (2005). Very fast two-dimensional NMR spectroscopy for real-time investigation of dynamic events in proteins on the time scale of seconds. *Journal of the American Chemical Society*, *127*(22), 8014–8015.

Schanda, P., Van Melckebeke, H., & Brutscher, B. (2006). Speeding up three-dimensional protein NMR experiments to a few minutes. *Journal of the American Chemical Society*, *128*(28), 9042–9043.

Schmieder, P., Stern, A. S., Wagner, G., & Hoch, J. C. (1993). Application of nonlinear sampling schemes to COSY-type spectra. *Journal of Biomolecular NMR*, *3*(5), 569–576.

Schubert, M., Kolbe, M., Kessler, B., Oesterhelt, D., & Schmieder, P. (2002). Heteronuclear multidimensional NMR spectroscopy of solubilized membrane proteins: Resonance assignment of native bacteriorhodopsin. *Chembiochem*, *3*(10), 1019–1023.

Schubert, M., Smalla, M., Schmieder, P., & Oschkinat, H. (1999). MUSIC in triple-resonance experiments: Amino acid type-selective (1)H-(15)N correlations. *Journal of Magnetic Resonance*, *141*(1), 34–43.

Schwarz, D., Junge, F., Durst, F., Frölich, N., Schneider, B., Reckel, S., et al. (2007). Preparative scale expression of membrane proteins in Escherichia coli-based continuous exchange cell-free systems. *Nature Protocols*, *2*(11), 2945–2957.

Senn, H., Eugster, A., Otting, G., Suter, F., & Wüthrich, K. (1987). 15N-labeled P22 c2 repressor for nuclear magnetic resonance studies of protein-DNA interactions. *European Biophysics Journal*, *14*(5), 301–306.

Serrano-Vega, M. J., Magnani, F., Shibata, Y., & Tate, C. G. (2008). Conformational thermostabilization of the beta1-adrenergic receptor in a detergent-resistant form. *Proceedings of the National Academy of Sciences of the United States of America*, *105*(3), 877–882.

Shin, J., & Noireaux, V. (2010). Efficient cell-free expression with the endogenous E. Coli RNA polymerase and sigma factor 70. *Journal of Biological Engineering*, *4*(1), 8.

Shortle, D. (1994). Assignment of amino acid type in ^{1}H-^{15}N correlation spectra by labeling with ^{14}N-amino acids. *Journal of Magnetic Resonance. Series B*, *105*, 88–90.

Shrestha, P., Holland, T. M., & Bundy, B. C. (2012). Streamlined extract preparation for Escherichia coli-based cell-free protein synthesis by sonication or bead vortex mixing. *BioTechniques*, *53*, 163–174.

Sobhanifar, S., Schneider, B., Lohr, F., Gottstein, D., Ikeya, T., Mlynarczyk, K., et al. (2010). Structural investigation of the C-terminal catalytic fragment of presenilin 1. *Proceedings of the National Academy of Sciences of the United States of America*, *107*(21), 9644–9649.

Stanek, J., Nowakowski, M., Saxena, S., Ruszczyńska-Bartnik, K., Ejchart, A., & Koźmiński, W. (2013). Selective diagonal-free (13)C, (13)C-edited aliphatic-aromatic NOESY experiment with non-uniform sampling. *Journal of Biomolecular NMR*, *56*(3), 217–226.

Staunton, D., Schlinkert, R., Zanetti, G., Colebrook, S. A., & Campbell, I. D. (2006). Cell-free expression and selective isotope labelling in protein NMR. *Magnetic Resonance in Chemistry: MRC*, *44*, S2–S9. Spec. No.

Sun, Z. Y., Frueh, D. P., Selenko, P., Hoch, J. C., & Wagner, G. (2005). Fast assignment of 15N-HSQC peaks using high-resolution 3D HNcocaNH experiments with non-uniform sampling. *Journal of Biomolecular NMR*, *33*(1), 43–50.

Takahashi, H., Odaka, A., Kawaminami, S., Matsunaga, C., Kato, K., Shimada, I., et al. (1991). Multinuclear NMR study of the structure of the Fv fragment of anti-dansyl mouse IgG2a antibody. *Biochemistry*, *30*(26), 6611–6619.

Tate, S., Kikumoto, Y., Ichikawa, S., Kaneko, M., Masui, Y., Kamogashira, T., et al. (1992). Stable isotope aided nuclear magnetic resonance study to investigate the receptor-binding site of human interleukin 1 beta. *Biochemistry*, *31*(8), 2435–2442.

Trbovic, N., Klammt, C., Koglin, A., Löhr, F., Bernhard, F., & Dötsch, V. (2005). Efficient strategy for the rapid backbone assignment of membrane proteins. *Journal of the American Chemical Society*, *127*(39), 13504–13505.

Tugarinov, V., Hwang, P. M., Ollerenshaw, J. E., & Kay, L. E. (2003). Cross-correlated relaxation enhanced 1H[bond]13C NMR spectroscopy of methyl groups in very high molecular weight proteins and protein complexes. *Journal of the American Chemical Society*, *125*(34), 10420–10428.

Tugarinov, V., Kanelis, V., & Kay, L. E. (2006). Isotope labeling strategies for the study of high-molecular-weight proteins by solution NMR spectroscopy. *Nature Protocols*, *1*(2), 749–754.

Tugarinov, V., & Kay, L. E. (2004). An isotope labeling strategy for methyl TROSY spectroscopy. *Journal of Biomolecular NMR*, *28*(2), 165–172.

Viegas, A., Viennet, T., & Etzkorn, M. (2016). The power, pitfalls and potential of the nanodisc system for NMR-based studies. *Biological Chemistry*, *397*(12), 1335–1354.

Vuister, G. W., Clore, G. M., Gronenborn, A. M., Powers, R., Garrett, D. S., Tschudin, R., et al. (1993). Increased resolution and improved spectral quality in four-dimensional 13C/13C-separated HMQC-NOESY-HMQC spectra using pulsed field gradients. *Journal of Magnetic Resonance. Series B*, *101*(2), 210–213.

Waberer, L., Henrich, E., Peetz, O., Morgner, N., Dötsch, V., Bernhard, F., et al. (2017). The synaptic vesicle protein SV31 assembles into a dimer and transports Zn(2). *Journal of Neurochemistry*, *140*(2), 280–293.

Weigelt, J., van Dongen, M., Uppenberg, J., Schultz, J., & Wikström, M. (2002). Site-selective screening by NMR spectroscopy with labeled amino acid pairs. *Journal of the American Chemical Society*, *124*(11), 2446–2447.

Werner-Allen, J. W., Coggins, B. E., & Zhou, P. (2010). Fast acquisition of high resolution 4-D amide-amide NOESY with diagonal suppression, sparse sampling and FFT-CLEAN. *Journal of Magnetic Resonance*, *204*(1), 173–178.

Westler, W. M., Stockman, B. J., Hosoya, Y., Miyake, Y., Kainosho, M., & Markley, J. L. (1988). Correlation of carbon-13 and nitrogen-15 chemical shifts in selectively and uniformly labeled proteins by heteronuclear two-dimensional NMR spectroscopy. *Journal of the American Chemical Society*, *110*(18), 6256–6258.

Wittekind, M., & Mueller, L. (1993). HNCACB, a high-sensitivity 3D NMR experiment to correlate amide-proton and nitrogen resonances with the α- and β-carbon resonances in proteins. *Journal of Magnetic Resonance. Series B*, *101*, 201–205.

Wu, P. S., Ozawa, K., Jergic, S., Su, X. C., Dixon, N. E., & Otting, G. (2006). Amino-acid type identification in 15N-HSQC spectra by combinatorial selective 15N-labelling. *Journal of Biomolecular NMR*, *34*(1), 13–21.

Yabuki, T., Kigawa, T., Dohmae, N., Takio, K., Terada, T., Ito, Y., et al. (1998). Dual amino acid-selective and site-directed stable-isotope labeling of the human c-Ha-Ras protein by cell-free synthesis. *Journal of Biomolecular NMR*, *11*(3), 295–306.

Yamazaki, T., Lee, W., Arrowsmith, C. H., Muhandiram, D. R., & Kay, L. E. (1994). A suite of triple resonance NMR experiments for the backbone assignment of 15N, 13C, 2H labeled proteins with high sensitivity. *Journal of the American Chemical Society*, *116*(26), 11655–11666.

Yang, W. C., Patel, K. G., Wong, H. E., & Swartz, J. R. (2012). Simplifying and streamlining Escherichia coli-based cell-free protein synthesis. *Biotechnology Progress*, *28*(2), 413–420.

Zawadzka-Kazimierczuk, A., Kazimierczuk, K., & Koźmiński, W. (2010). A set of 4D NMR experiments of enhanced resolution for easy resonance assignment in proteins. *Journal of Magnetic Resonance*, *202*(1), 109–116.

Zhao, L., Wang, S., Run, C., OuYang, B., & Chou, J. J. (2016). Specific lipid binding of membrane proteins in detergent micelles characterized by NMR and molecular dynamics. *Biochemistry*, *55*(38), 5317–5320.

Zubay, G. (1973). In vitro synthesis of protein in microbial systems. *Annual Review of Genetics*, *7*, 267–287.

Zuiderweg, E. R. P., Petros, A. M., Fesik, S. W., & Olejniczak, E. T. (1991). Four-dimensional [^{13}C, ^{1}H, ^{13}C, ^{1}H] HMQC-NOE-HMQC NMR spectroscopy: Resolving tertiary NOW distance restraints in spectra of larger proteins. *Journal of the American Chemical Society*, *113*, 370–372.